Numerical and Experimental Study of the Deformation of Gray Cast Iron Plates

NUMERICAL AND EXPERIMENTAL STUDY OF THE DEFORMATION OF GRAY CAST IRON PLATES

BY

KHURRAM IQBAL, M. A. Sc.

A THESIS

SUBMITTED TO THE DEPARTMENT OF MECHANICAL ENGINEERING

AND THE SCHOOL OF GRADUATE STUDIES

OF MCMASTER UNIVERSITY

IN PARTIAL FULFILMENT OF THE REQUIREMENTS

FOR THE DEGREE OF

MASTER OF APPLIED SCIENCE

Master of Applied Science (2009) McMaster University

(Mechanical Engineering) Hamilton, Ontario, Canada

TITLE:	Numerical and Experimental Study of the Deformation of Gray Cast Iron Plates
AUTHOR:	Khurram Iqbal M. A. Sc, (Mechanical Engineering) McMaster University, Hamilton, Canada
SUPERVISOR:	Dr. Mohamed. S. Hamed
CO-SUPERVISOR:	Dr. A. A. Hassan Ali
NUMBER OF PAGES:	xvii, 87

TO

Abbu and Ammi

Contents

Abstract

Helical heating coils are widely used in most conventional electric stoves for many years, these heating coils can reach 600-700°C, which is higher than the ignition point of oil and grease (about 400°C), leading to many fires. Pioneering Technology Inc. has developed a Safe-T Element plate to address such problem. The Safe-T Element plate is manufactured from Gray Cast Iron. However, these plates deform during its use. This study was carried out to investigate the current Safe-T Element design, both experimentally and numerically, in order to determine the root causes behind the deformation problem of the plate, and to suggest changes to the existing design in order to limit its distortion to acceptable targets.

A chemical analysis was carried out to establish the type of material of the Safe-T Element plate. Chemical analysis showed that the material of the plate is cast iron. The microstructure of the plate was tested in order to examine its type and homogeneity Tensile testing was carried to establish the grade of the material, and to calculate the value of its young's modulus and yield strength. Tensile testing indicated that the material of the Safe-T Element plate is close to Gray Cast Iron Class 40. Differential scanning calorimetry testing was carried out to investigate thermal stability of the plate material. This test indicated that material is thermally stable.

Thermal cycling testing indicated that the root cause of the deformation problem is elastic thermal buckling. Temperature uniformity tests were carried out. More than 100 °C temperature variation in the radial direction was observed

To address the distortion of the plate, an optimum geometry has been suggested based on the findings of the numerical investigation by removing the outer ring from the original design of the plate.

Acknowledgment

First and foremost, I thank Almighty God for everything given to me.

I would like to express my deep and sincere gratitude to my supervisor, Dr. Hamed, Associate Professor, Department of Mechanical Engineering, McMaster University for being my mentor and guide throughout my student life at McMaster University. His knowledge and logical way of thinking has been of precious help to me. I want to thank Dr. Hamed for his patience and the time and energy he spared for me during the period of my research at McMaster University. I would like to express my thanks to my co-supervisor, Dr. Hassan Ali for helping me directly and indirectly in accomplishing this project and giving me a learning environment to grow personally as well as professionally.

I wish to express my warm and sincere thanks to my instructors at McMaster University, Dr. Shankar, Dr. Lightstone and Dr. Judd for providing the technical knowledge base. I am grateful to Dr. Habibi for his support.

I also owe my heart-felt gratitude and thanks to Pioneering Technology Inc (PTI) for giving me the opportunity to work on their project. Special thanks to Ms. Mary and Mr. Peter from PTI.

During this work I have collaborated with many colleagues for whom I have great regard, and I wish to extend my warmest thanks to all those who have helped me with my work in the Department of Mechanical Engineering. I would like to thank Dr. Mike from MMRI, Material Science Department, McMaster University for his support.

My special gratitude is due to my brother, my sisters and their families for their loving support. My loving thanks are due to my friend Nasreen for all her support. I want to thank my beloved father for all the pain he endured and the life-long efforts he put up for our education. I am grateful to my mother and my fiancée for all the prayers they do for me and Sana, I love you.

List of Figures

List of Tables

Chapter 1

1 Introduction

1.1 Background

The radiant coil cook top used in conventional kitchen ranges is one of the most common and economical technology presently available. Precisely because this technology is economical, it has been in use for many years in multi-residential and senior housing communities.

But there is a major safety issue related to this technology. The temperature of a radiant coil element can reach up to 650°C, so that if a drop of oil spilled on a radiant cooking coil, oil temperature can reach its ignition temperature (400-450°C) and it can accordingly ignite (Figure 1.1), causing fire.

Despite the continuous efforts of the Fire Prevention Association (NFPA) and the U.S. Fire Administration (USFA), stovetop cooking related fires continue to be the number one cause of fire in North America sometimes resulting in calamitous deaths and significant loss of property.

Figure 1 1 Cooking pot left unattended on the normal Stove causing fire due to ignition in the cooking oil [1]

1.2 Technical Solution

1.2.1 Safe-T Element plate -an innovative technology developed by Pioneering Technology Inc (PTI), ON, Canada

Over the past five years, stove manufactures have been motivated by the Consumer Product Safety Commission to come up with a solution to this particular cause of fire.

PTI has thus developed the Safe-T Element plate which is a circular plate mounted on the top of existing radiant cooking coil as shown in Figure 1.2. The plate is cast from Grey Cast Iron and equipped with a temperature control circuit to limit its temperature to 350 °C - 400 °C for regular cooking purposes. This technology prevents cooking related fires by avoiding direct contact between the cooking oils and the surface of radiant heating elements. Energy consumption is also

reduced because of stovetop on and off heating cycle (as explained later) during the cooking process which in turn reduces the amount of electricity required as stated by PTI [1]

Figure 1.2. PTI's Safe-T Element plate mounted on a radiant heating element [1]

This innovative technology of the Safe-T Element plate has become very popular The impact of this product is very substantial, even in its initial stage of launching, considering the appliances market that is being targeted (5.6 billion USD in US only).

The United States Air Force (USAF) has reviewed the suitability of the Safe-T Element technology for commercial Air Force Base (AFB) applications and has determined that the technology is acceptable as an alternative means of compliance with their UFC 3-600-01 military code requirement for a range fire safety system [1]

Housing societies like Rhode Island's Providence Housing Authority (PHA) is presently using the Safe-T Element Technology on the recommendation of the prestigious U.S. Department of Homeland Security's Federal Emergency Management Agency [1].

1.2.2 Problem encountered with the Safe-T Element plate

While the benefits of the Safe-T Element plate are obvious, there is one major technical problem that has been encountered which is the deflection of the plate due to heating. Due to this, the plate does not remain flat and horizontal, which reduces the contact area between the plate and the pot placed on top of it from one side and the plate and the radiant heating coil from the other side. This causes unacceptable long cooking times due to reduction of heat transfer from the coil to the pot.

1.3 Objective of the Present Research

The objective of the present study is to investigate both experimentally and numerically the cause of the deformation of the Safe-T Element plate during a typical heating cycle and to propose a solution to the deformation problem aiming to achieve a maximum deformation of less than 0.1 mm, as recommended by the industrial partner, Pioneering Technology Inc to enhance performance of the Safe-T Element plate.

1.4 Background and literature Review

1.4.1 Material of the Safe-T Element:

In order to determine the type of Gray Cast Iron used for casting the Safe-T Element plates, first it is important to understand some basics about Cast Iron.

Gray Cast Iron is one of the four types of Cast Iron [2]. These four types of Cast Iron are [3]

1 Gray Cast Iron
2. Ductile Cast Iron
3. White Cast Iron
4. Malleable Cast Iron.

The type depends on the shape of graphite present in the metal (iron) matrix. Figure 1.3 shows, optical photomicrographs of the different types of Cast Iron [4].

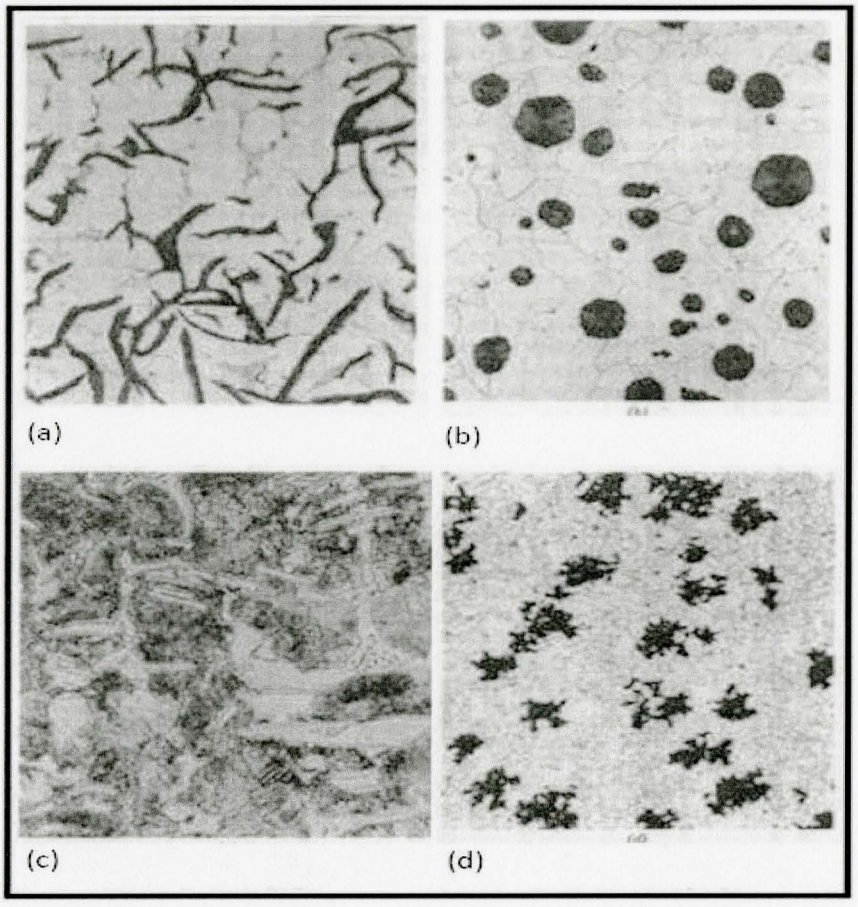

Figure 1.3 Microstructure of various types of Cast Iron [4]

Figure No 1.3a shows the dark graphite flake embedded in a ferrite matrix at 500X magnification of Gray Cast Iron.

Figure No 1.3b dark graphite nodule in a ferrite matrix at 200X magnification in the Ductile Cast Iron.

Figure 1.3c shows the light cementite regions surrounded by the Pearlite matrix at 400X magnification in the White Cast Iron.

Figure 1.3d shows the dark graphite rosettes in a ferrite metal matrix at 150X magnification in the Malleable Cast Iron.

1.4.2 Factors leading to different types of Cast Iron

The properties of Cast Iron are very much dependent on the manufacturing process. The factors leading to different types of Cast Iron are: (1) chemical composition, (2) Inoculation, (3) cooling rate and (4) section thickness [5]. Inoculation is a small quantity of an element added to the molten metal. These small quantities of additives are added to the molten metal just before it is poured in the mould in order to achieve the desired shape of the graphite in the final product [6]. There is a set of elements known as Inoculation elements having tendency to make the shape of graphite round in the Ductile Cast Iron and in the form of flake in the Gray Cast Iron.

The elements which could be used for the nodularizing (tendency to make shape round) of the graphite are magnesium, cerium and calcium [8]. Other elements have a greater tendency to arrest the growth of graphite, such as sulphar, nitrogen and oxygen [9]. Less than 0.005 percent of Boron can lead to a hard white ironing surface on the casting.

The cooling rate and thickness of the section also affects the microstructure of the Gray Cast Iron. The rate of solidification is different for the varying section thickness in the same casting. Due to this, there will be different shapes of graphite leading to different properties in the finished product even though casting has the same molten material [10]. This difference in the metal matrix and the graphite shape is the basic criteria for the different types of Cast Iron [4].

1.4.3 Understanding the Mechanism of Formation of Different Metal Matrices and Graphite Shape in the Gray Cast Iron

Gray Cast Iron composition ranges from 2.5 to 4% carbon, 1 to 3% silicon and 0.4 to 1% manganese [9]. The other two elements traditionally present in the Gray Cast Iron are Sulfur and

Phosphorus [8]. During the eutectic reaction three dimensional graphite flakes dispersed in the ferrite, pearlite, or other from the austenite forms during the solidification [6]. Due to the rate of cooling and the presence of materials like Silicon, the eutectic reaction has the following two different possibilities [9]

1. Liquid = Austenite + Cementite (Fe3C)
2. Liquid = Austenite + Graphite

The final microstructure of the Safe-T Element plate made from Gray Cast Iron could have a carbon-rich phase being graphite or cementite (Fe3C) [9]. The formation of graphite can be promoted through slow cooling, high carbon and silicon contents, larger section size and the presence of inoculation favoring the formation of graphite [9].

In the Iron Carbon phase diagram shown in Figure 1.4, at a temperature above the eutectoid, if the cooling is fast, the pearlitic matrix will form. If the cooling is slow, ferritic Gray Cast Iron will form. In the case if the matrix has both ferritic and pearlitic structure, then the Ferrite will be formed near the flake and the rest of the metal matrix is Pearlite. Ferritic is soft whereas pearlitic is the strongest, as far as the strength is concerned [2].

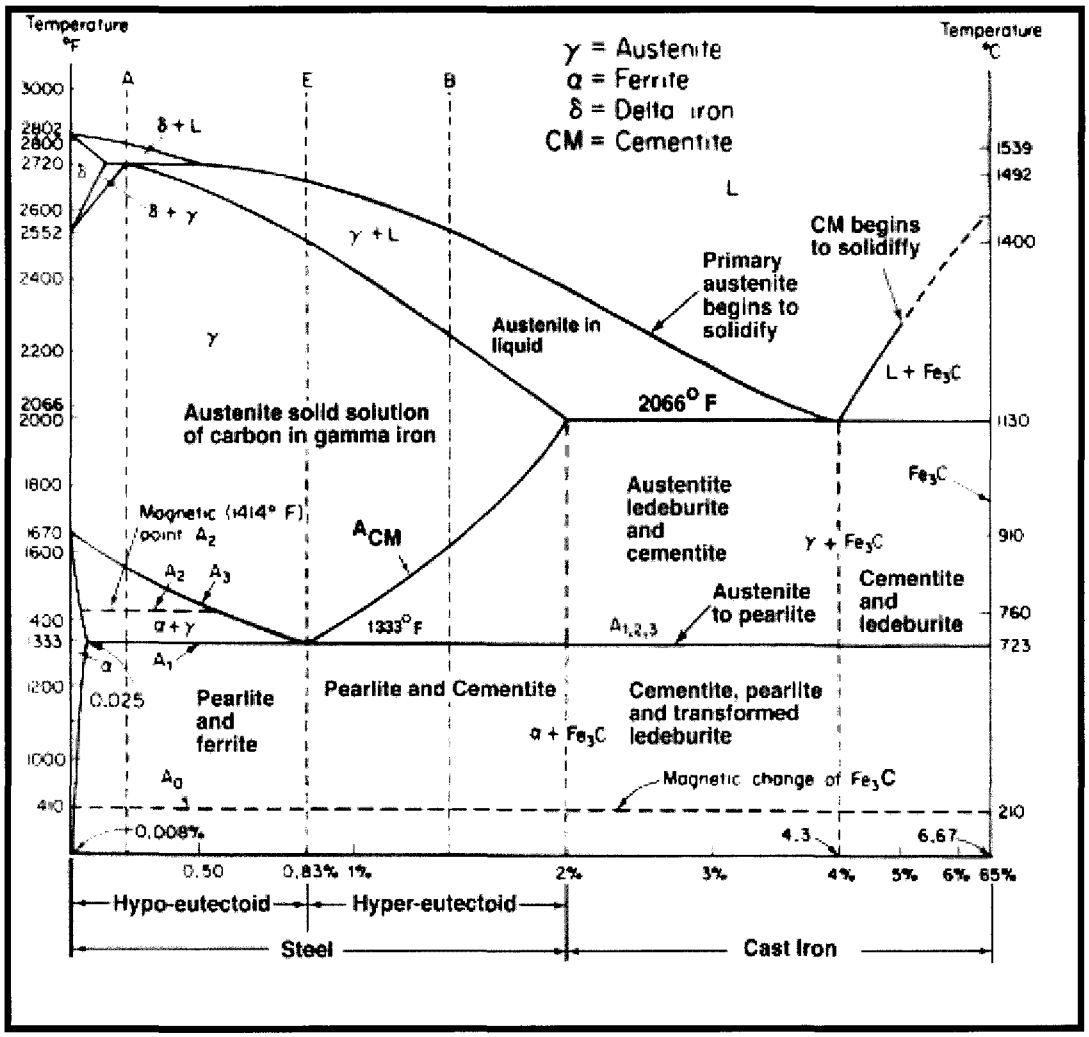

Figure 1.4: Iron Carbon Phase Diagram [10].

It can be observed as well that at 1540°C almost 6 percent carbon is soluble in the Iron, but as the Iron cools and reaches 1148°C, only 2 percent carbon is soluble in the Iron and when an equilibrium condition is reached, excess carbon is forced out of the solution [4].

When carbon is added to Iron, they form carbide of Iron known as cementite (Fe_3C) [11]. Iron without carbon is known as ferrite and has a body-centered crystal structure [11]. If more carbon is added and fast cooling is carried out while solidification of molten material, then an alternating

plate of Iron-carbide and ferrite make up the Pearlite matrix adjacent to carbon. This Pearlite matrix has higher strength and hardness than the ferrite matrix. If the graphite is converted to the spherical form, the flake size present in the Gray Cast Iron will lead to a reduction in the internal stress and its mechanical property. But, at the same time, this will reduce the thermal conductivity of the material which is an important property for the performance of the Safe-T Element plate [12].

1.4.4 Advantage of using Gray Cast Iron as a Material for the Safe-T Element plate

The selection of Gray Cast Iron for the Safe-T Element is due to:

1. Gray Cast Iron is economical and inexpensive.
2. It has a low melting point and a high fluidity that makes Gray Cast Iron easy to cast especially to make a ring around the core base of the Safe-T Element plate.
3. Gray Cast Iron is also very popular due to its excellent machinibilty, bearing properties, good damping properties, wear resistance and also because it is good for thermal application [13].

Gray Cast is one of the most regularly used materials [5]. At present, it has been estimated that its total annual production is many times the total production of all other cast alloys in the world.

1.4.5 Classification of Gray Cast Iron

Gray Cast Iron is generally classified according to the ASTM A48 classification system. Classes range from 20 to 80 [14]. Each class represents the tensile strength of the particular class, for example ASTM A 48 class 40 has 40,000 psi tensile strength [2].

Gray Cast Iron is generally characterized by its tensile strength [2] as it has almost negligible ductility.

Gray Cast Iron is influenced by a reduction in area and at the same strain the stress level goes up with an increase in the reduction of the area of the specimen [15], and consequently increasing the maximum tensile strength, which in turn affects the way the Gray Cast Iron, is graded.

Gray Cast Iron is also sensitive to the orientation of the graphite flake. If the graphite flake is oriented in the direction of the applied force, this will increase the loading area and in turn the tensile strength which is one of the criteria for grading Gray Cast Iron [15]. Alternatively, if the orientation of these graphite flakes is in opposite direction to the applied force, this will lower the tensile strength. Gray Cast Iron mainly consists of preferentially or randomly oriented flakes of graphite of different shapes and sizes depending on the way the casting has been carried out, dispersed in an Iron matrix. These graphite flakes are the main reason for the improvement in the thermal conductivity of the Gray Cast Iron though it causes the point of stress concentration due to sharp edge of the flakes and leads to discontinuity [16]. If Gray Cast Iron experiences repeated heating and cooling in oxidizing atmosphere, oxides are developed inside the crystal structure [17]. Mechanical properties of Gray Cast Iron depend on micro-structure parameters like the amount of graphite and the content of ferrite [12].

For Gray Cast Iron, high graphite content with randomly oriented graphite flakes lowers the young's modulus and raises its thermal conductivity. The tensile strength of Cast Iron can be improved by reducing the carbon/silicon ratio, but this will lead to a reduction in the thermal conductivity of the material. In the case of Gray Cast Iron, lower tensile strength combined with a lower hardness and increase in the percentage of graphite leads to better machinibilty for the Cast Iron. The greater quantity of graphite present in the matrix favors the disappearance of the micro-porosities, which may be caused by the solidification contraction or by instability in the modulus when pouring the metal.

The variation of the thermal diffusivity of eight different samples of Gray Cast Iron as a function of temperature is shown in Figure 1.5 [2]. For the same sample made of Gray Cast Iron, it can be observed that as temperature increases, the value of thermal diffusivity decreases significantly.

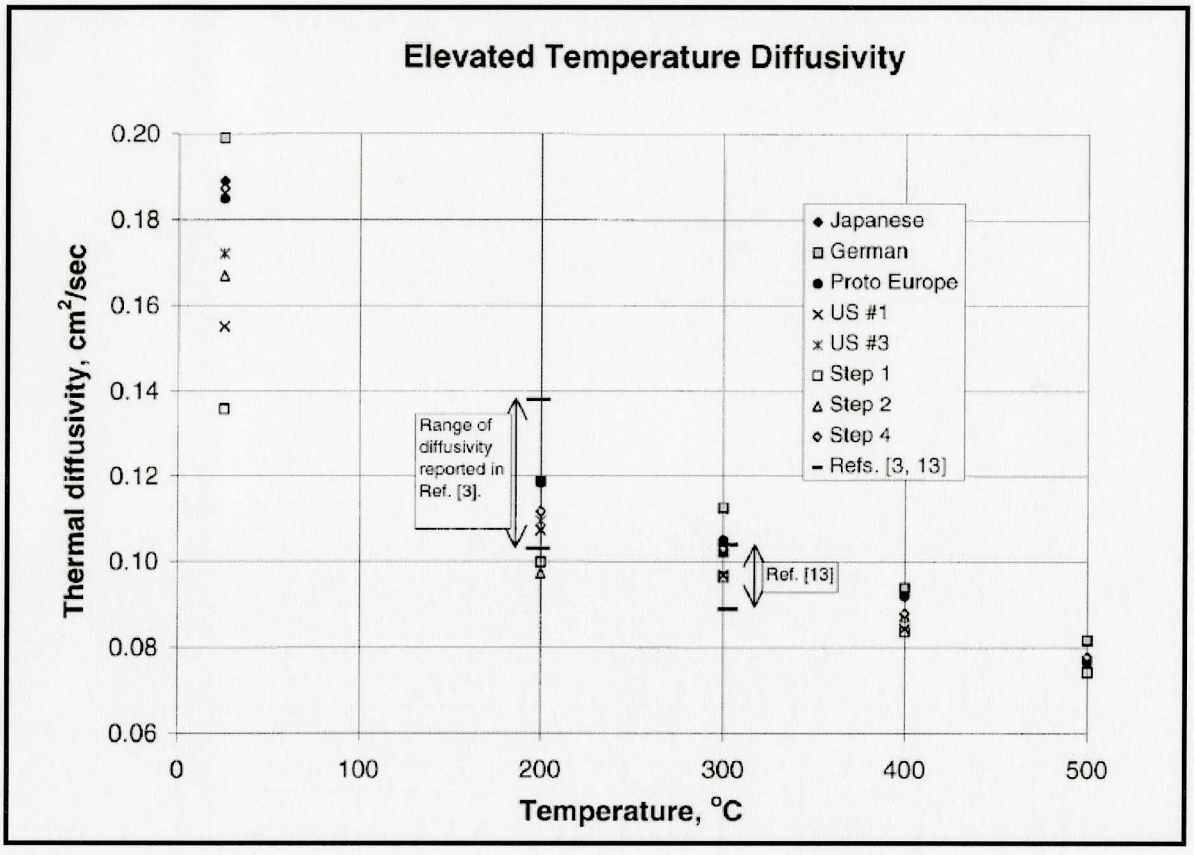

Figure 1.5 Thermal diffusivity of Gray Cast Iron as a function of temperature [18]

Figure 1.6 shows thermal diffusivity of Gray Cast Iron as a function of the Graphite Aspect Ratio [2] Even with the same chemical composition, the graphite aspect ratio could vary because of different cooling rates leading to a different property for the material chosen for the Safe-T Element plate.

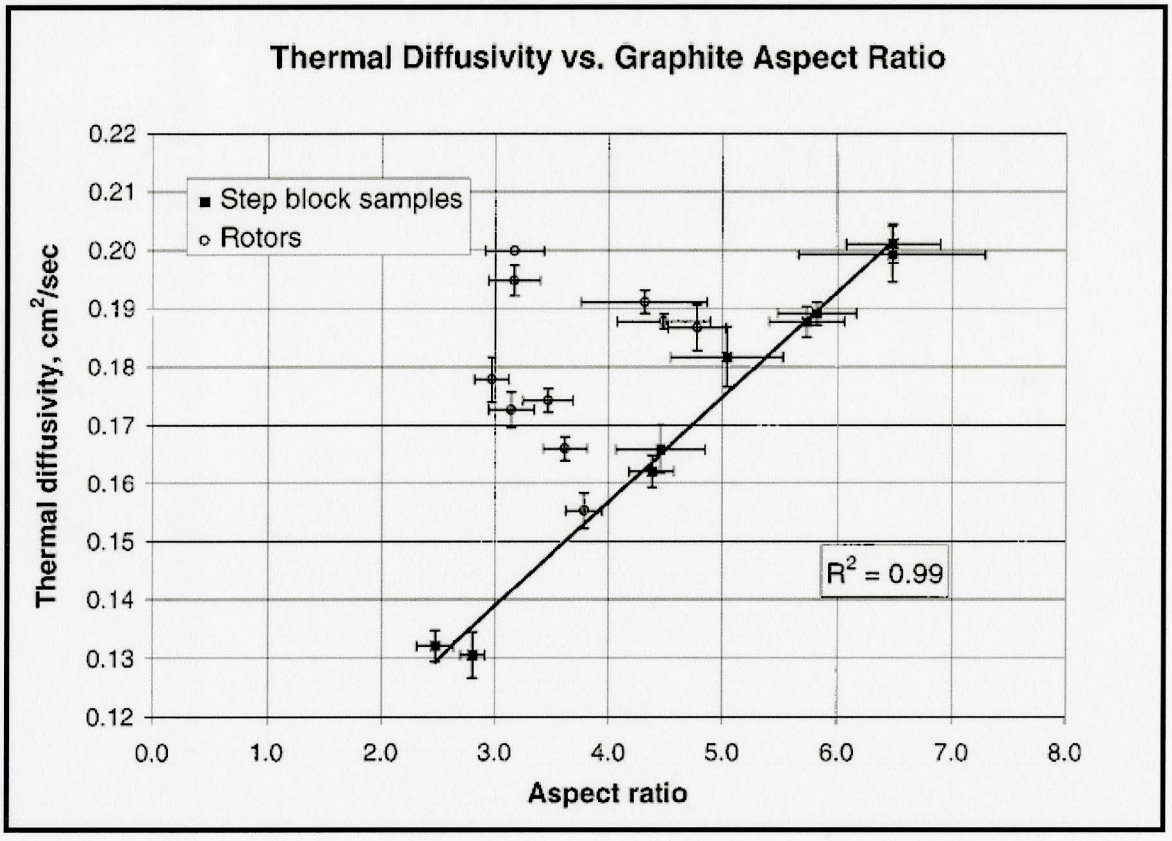

Figure 1.6: Thermal Diffusivity of Gray Cast Iron as a function of Graphite Aspect Ratio [18].

The effect of carbon equivalence on thermal diffusivity of Gray Cast is shown in Figure 1 7 It can be observed in Figure 1 7 that at room temperature thermal diffusivity increases with an increase in the Carbon Equivalence [18] This carbon equivalence in turn depends on the chemistry of the material.

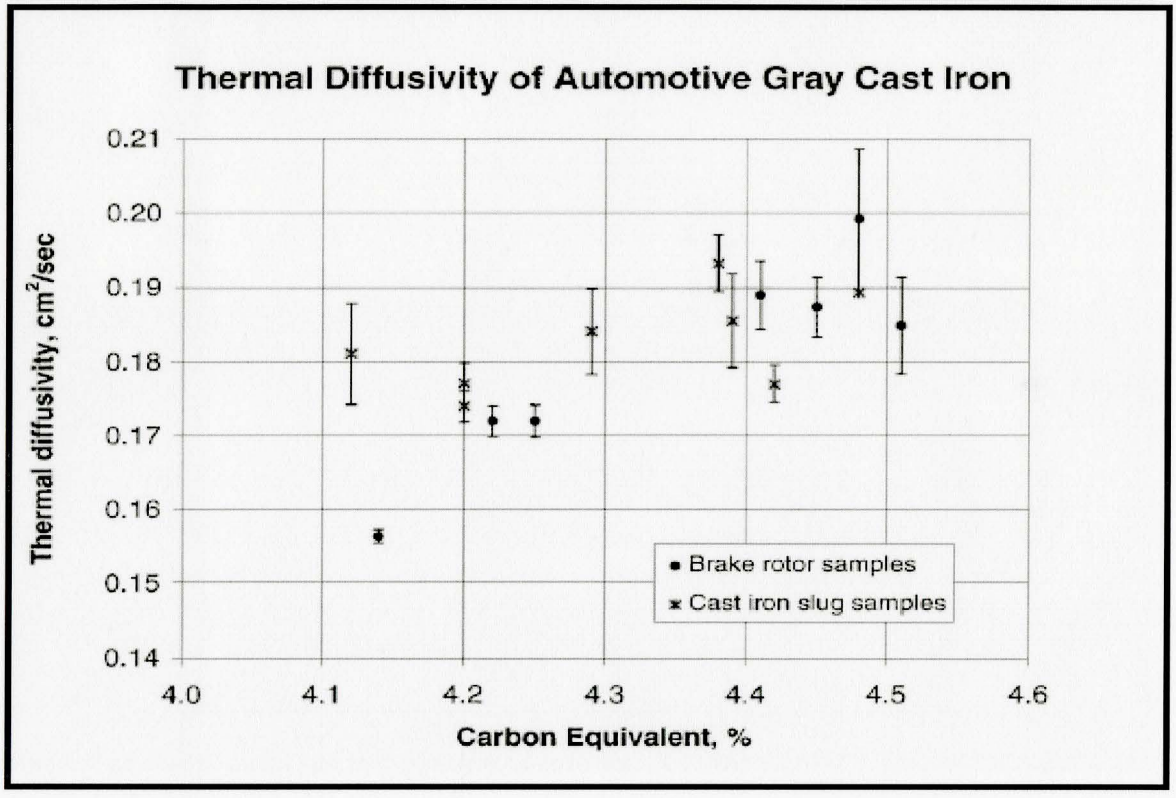

Figure 1 7 the effect of carbon equivalence on thermal diffusivity of Gray Cast Iron [18]

1.4.6 Challenges encountered due to graphite shape in the Safe-T Element plate

The two major factors on which the thermal and mechanical properties of the Safe-T Element plate depend are the size and the shape of the graphite. This makes the material of a Safe-T Element very challenging as the formation of Graphite and its shape and size depends on other factors like cooling which in turn depends on the section size and Inoculation [5] Gray Cast Iron is a unique material as far as Hooke's law is concerned.

Gray Cast Iron deviates from the linear behavior of Hooke's law [19] Hooke's law cannot be applied to Gray Cast Iron due to non linear relationship between stress and strain [3]. The reason

for this deviation can be attributed to the graphite present in the Gray Cast Iron matrix causing stress concentration due to the heterogeneity. This heterogeneity is caused by a metallic matrix distributed in graphite lamellae [20].

1.4.7 Available properties found in the literature for Grade 40 of Gray Cast Iron

The thermal and mechanical properties of Gray Cast Iron such as the coefficient of linear expansion, Young's modulus, Yield strength, Poison's ratio are required as a function of temperature to carry out any numerical investigation. Values of the thermal conductivity and the heat capacity are also required.

As it has been already explained in the previous section that the properties of Cast Iron not only depend on the percentage of the carbon present but also on other parameters like section size and Inoculation [21]. All these parameters on which the properties depend on make it very difficult to find the proper set of properties of Gray Cast Iron.

Not all properties of Gray Cast Iron are available in the literature. Establishing the properties of Cast Iron at high temperatures in a detailed and systematic manner is a recent area of research. Gray Cast Iron manufacturing process has evolved over a period of time and its products are difficult to reproduce due to dependence on cooling rate. Even if the chemical composition is the same, a slight variation in the method may lead to different properties of the finished product [14].

The available high-temperature data for Gray Cast Iron is limited in scope and available in bits and parts. Even if data is available, there is a variation because of different test methods and

raw materials used. Figure 1.8 shows stress, strain curve of class 40 Gray Cast Iron at various temperatures [2]

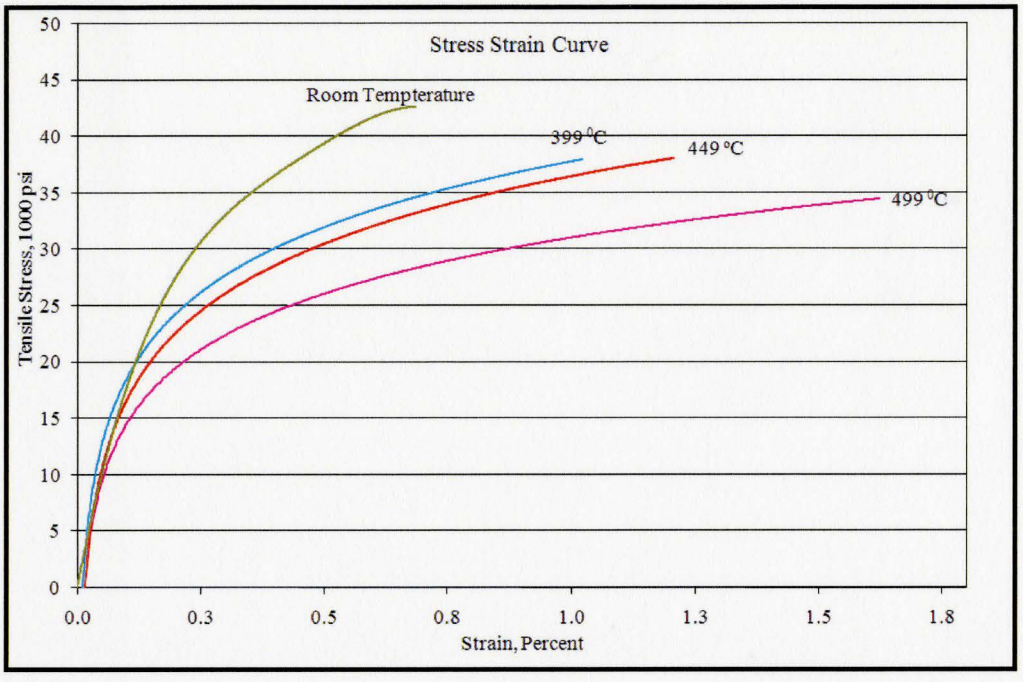

Figure 1.8 Variation of tensile stress with Strain of Gray Cast Iron at different temperatures [2]

Table 1 1 Tensile strength and Young's Modulus as a function of the temperature for Class 40 of Gray Cast Iron [2]

Temperature	Room	750F	840F	930F
Tensile Strength	42,000	39,000	38,000	31,000
Elongation Percent	0.74	1.23	1.30	1 75
Young's Modulus	18.5	18	16	15.5

Table 1.1 shows some properties of Gray Cast Iron at different temperature. As shown, as the temperature increases, the value of the tensile strength and Young's Modulus subsequently decreases.

Figure 1.9 shows the value of the coefficient of expansion as a function of temperature for class 40 of Gray Cast Iron [22]. As shown, the coefficient of expansion is a direct function of temperature.

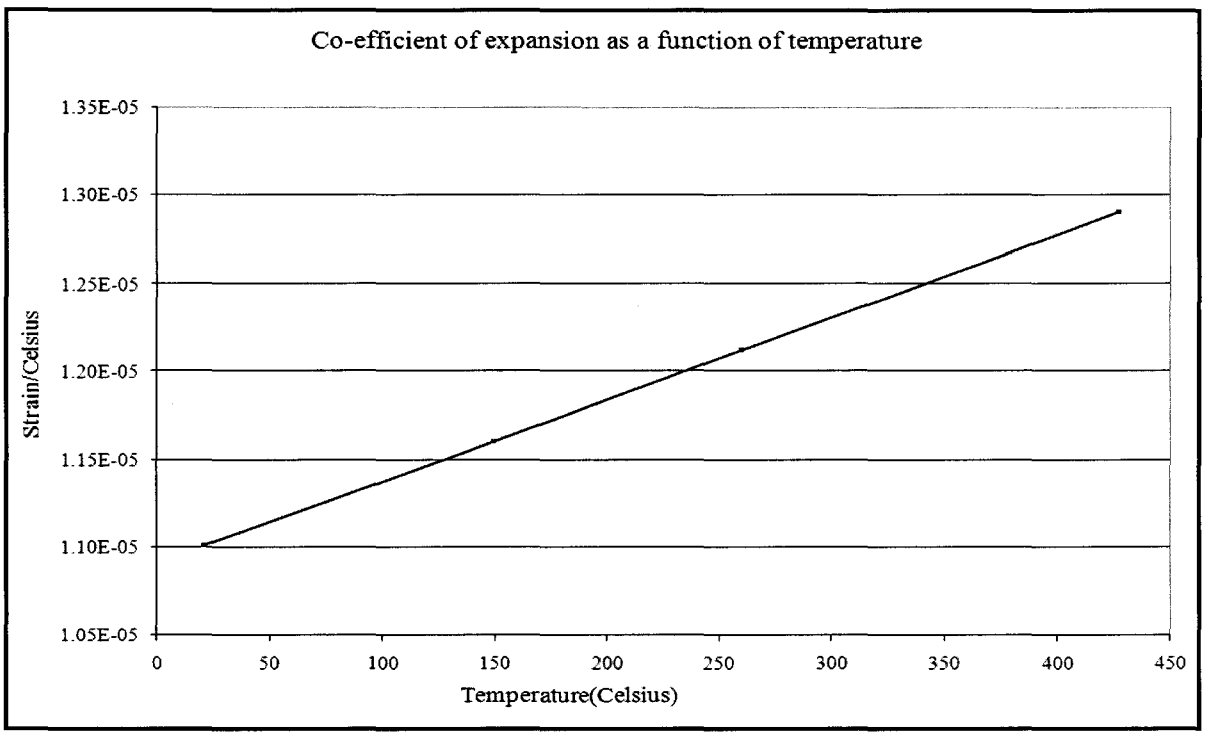

Figure 1.9: Coefficient of Expansion as a function of the temperature for Class 40 of Gray Cast Iron [24].

Figure 1.10 shows the thermal conductivity as a function of temperature [23]. It can be observed in Figure 1.10 that the thermal conductivity decreases as the temperature increases up to about 780°C.

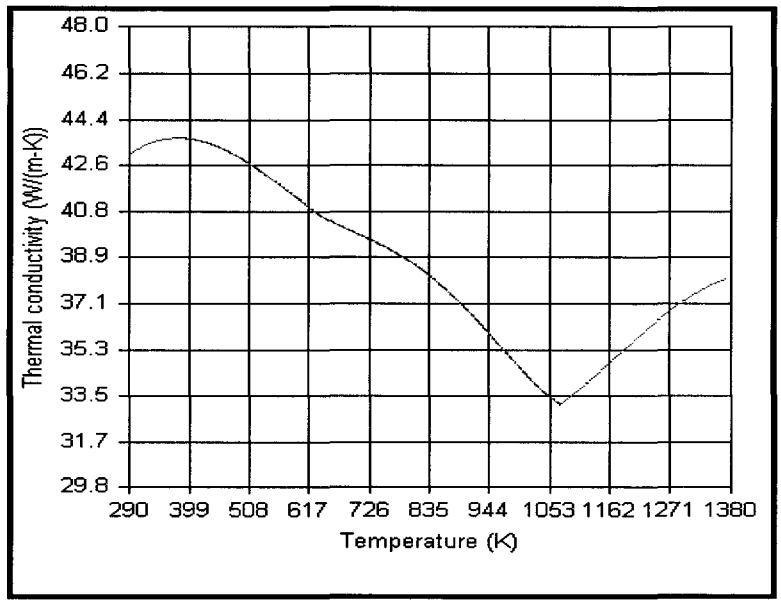

Figure 1.10: Thermal conductivity as a function of temperature of Class 40 of Gray Cast Iron [23].

Chapter 2

2 Experimental Setup

2.1 Introduction and Background

The objective of the experimental setup is to measure both the maximum deflection and the temperature in both the radial and circumferential directions along the Safe-T Element during a typical controlled heating cycle (200-400°C) of the Safe-T Element plates manufactured by two different manufacturers.

An Experimental Setup has been built to investigate the thermal deformation of samples of the Safe-T Element plate. Pioneering Technology has developed a patented technology for a controller that restricts the maximum temperature to 400°C for the Safe-T Element plate and leads to repeatable continuous on and off operation of the heating element. Due to this built-in controller, the overheating of the pot is prevented.

The shape of the Radiant Heating Element is helical as shown in Figure 2.1 This helical shaped Radiant Heating element is fixed in direct contact with the Safe-T Element plate using three clips. As shown in Figure 2.1, the entire area of the Safe-T Element plate is not in direct contact with the radiant heating element. This causes non-uniform heating of the Safe-T Element plate and leads to a large temperature difference across the Safe-T Element plate.

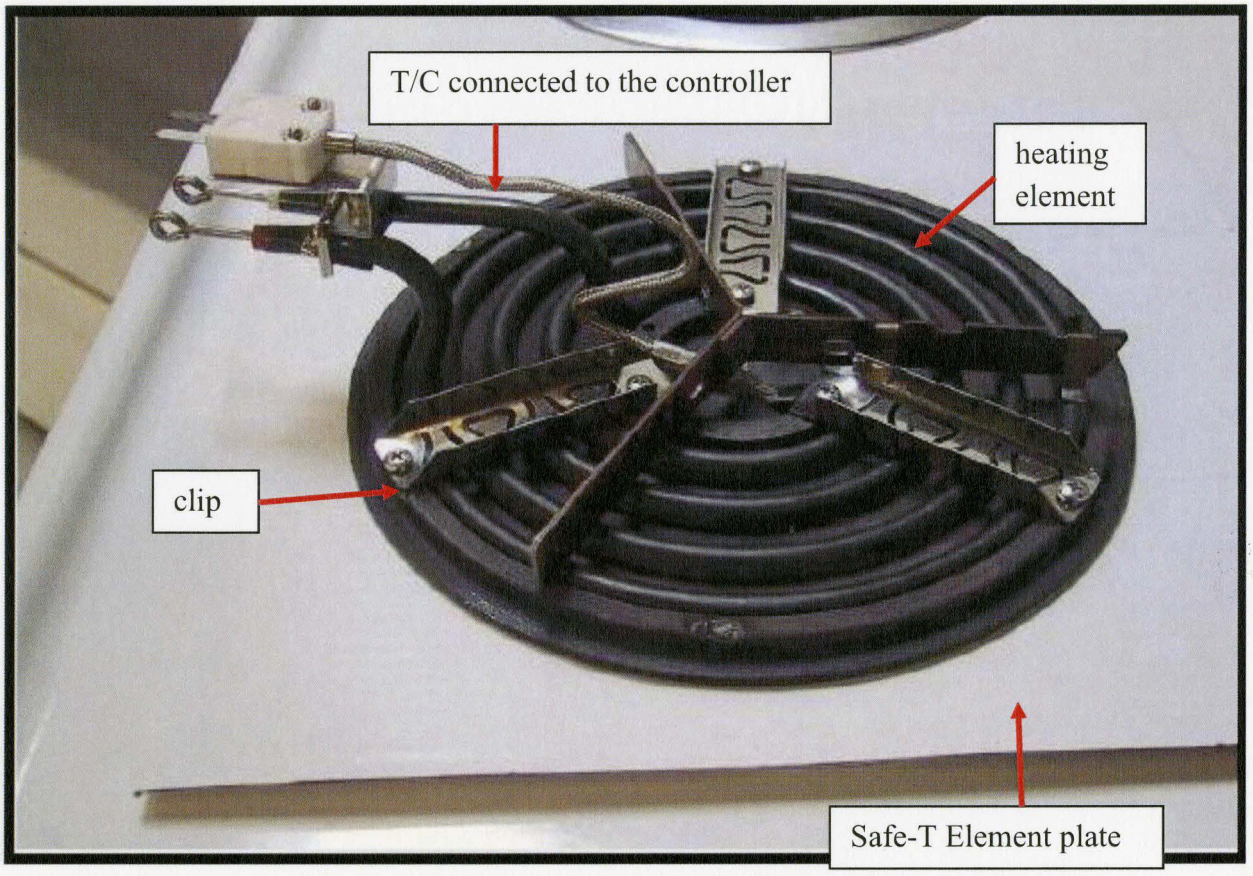

Figure 2.1 The Safe-T Element plate connected to a heating element [1]

Due to the non-uniform heating, a large temperature gradient in both the radial and circumferential directions of the Safe-T Element plate is expected. Since the Safe-T Element plate works in the temperature range of 200-400°C for the purpose of efficient cooking, this temperature range has been chosen as the temperature range for the experiments.

It is important to measure the temperature distribution in both the radial and circumferential directions to determine the temperature variation across the Safe-T Element plate. This temperature profile will be used in the numerical investigation to study the deflection remedy of the Safe-T Element plate.

2.2 Experimental Setup

The major components of the experimental setup are the temperature controller, the stove, the Safe-T Element plate, the radiant heating coil, data acquisition system and the computer, as shown in Figure 2.2.

Fourteen type K thermocouples have been mounted on the Safe-T Element plate and the temperature was recorded by using a Fluke data acquisition system shown in Figure 2.3. This data acquisition system has been further connected to the computer, where real time recording of temperatures can be performed.

The built-in controller of the stove has been bypassed and another controller shown in Figure 2.4 was used in order to carry out experiments at maximum heating capacity of the radiant coil heating element. The built-in controller limits the temperature of the Safe-T Element to 400°C.

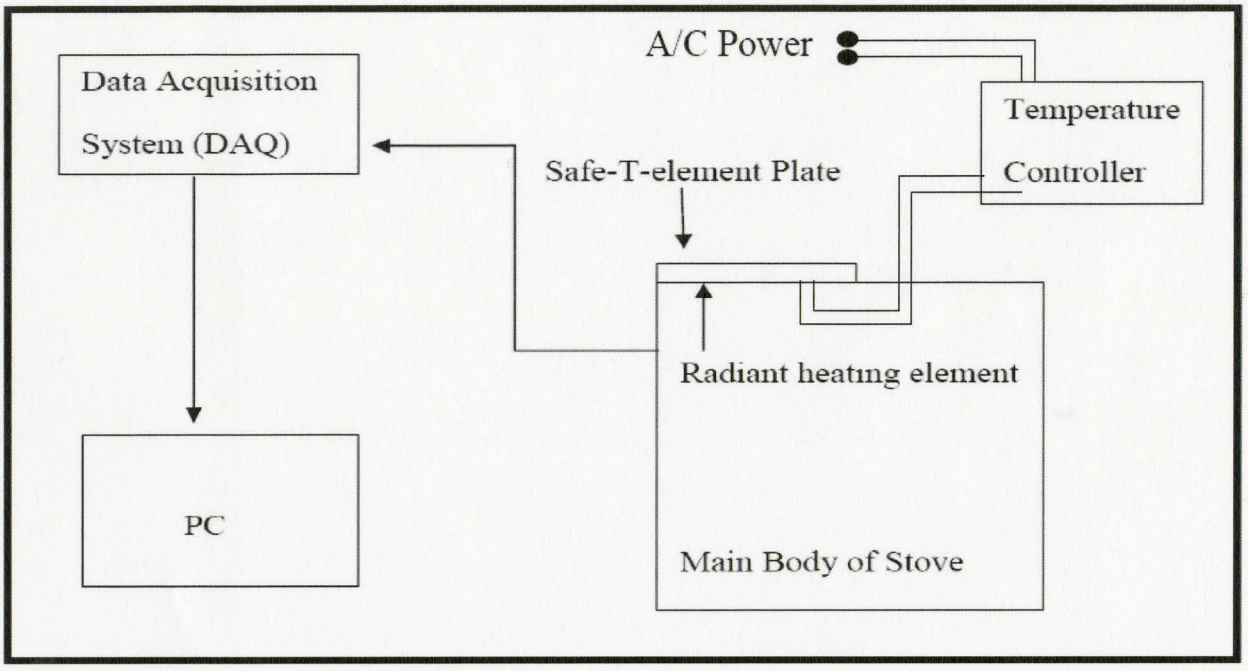

Figure 2.2. Schematic of the experimental setup showing all major components

Figure 2.3 Fluke data acquisition system

Figure 2.4. External temperature controller used in the experiments.

2.3 Thermocouple Mounting

Thermocouples were mounted in different stages. Initially, the thermocouples had been mounted between the radiant coil heating element and the Safe-T Element plate using small clips.

These clips have been made in such a way to leave a large groove in the clip, which allows the sliding motion in the vertical direction as shown in Figure 2.5 This arrangement gives some flexibility in fixing the thermocouples on the Safe-T Element plate. Through the help of these clips mounted on the support plate of the heating plate, the thermocouples could be rigidly fixed at the desired location of the Safe-T Element plate.

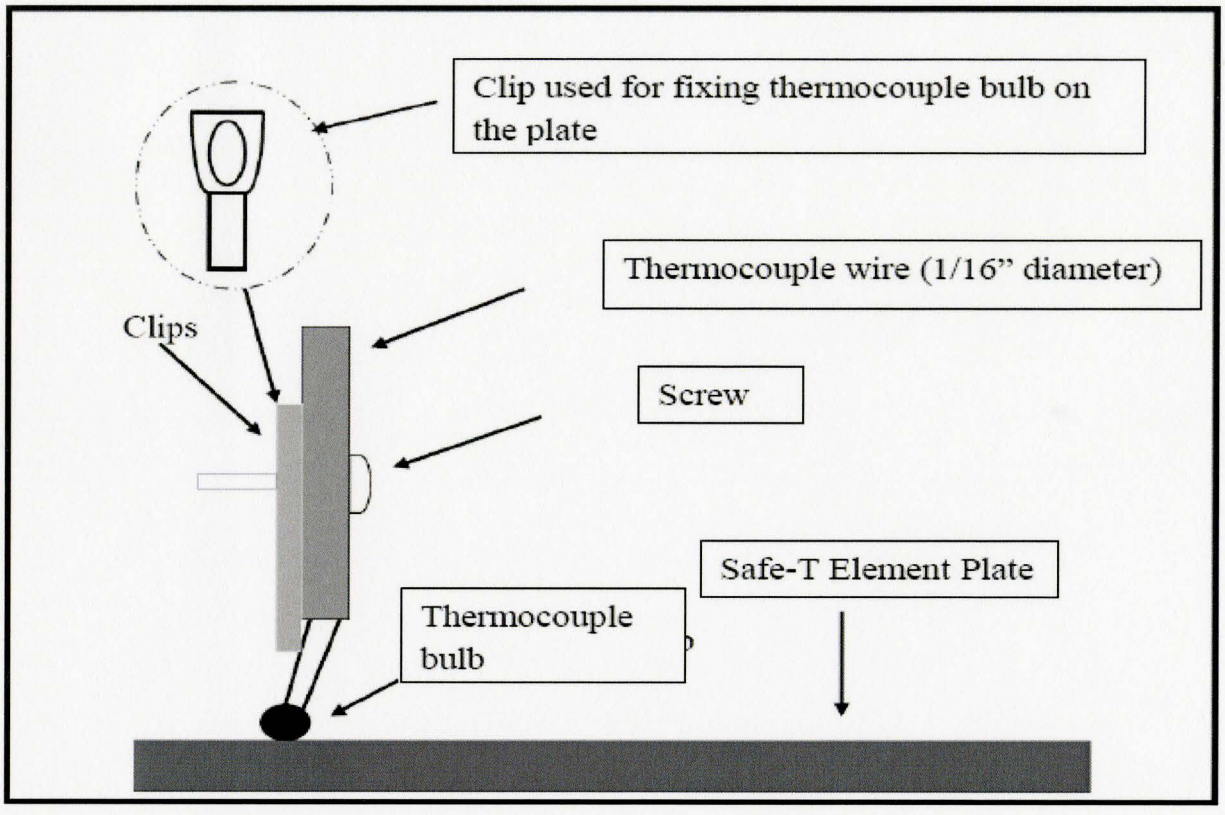

Figure 2.5 Mounting of thermocouples on the Safe-T Element plate

Initially, seven thermocouples were mounted as shown in Figures 2.5 and 2.6 on the Safe-T Element plate, in this way 22 plates from two different suppliers of Pioneering Technology Inc. had been tested and thermal profiles for these plates were generated.

Later, in the second stage of the temperature distribution measurement, the number of thermocouples was raised to 12 in order to have better understanding of the temperature distribution across the plate. The locations of the previous seven thermocouples have been kept the same.

In the third stage, a new set of experiments has been conducted in order to accurately measure the transient temperature distribution of the plate in both the radial and circumferential directions. Now, instead of using clips, the thermocouples were embedded inside the Safe-T

Element plate in order to avoid any radiation effects from the heater and to give an accurate representation of the plate temperature variation.

Figures 2.6 show the locations of the thermocouples mounted on the plate for measuring the temperature distribution.

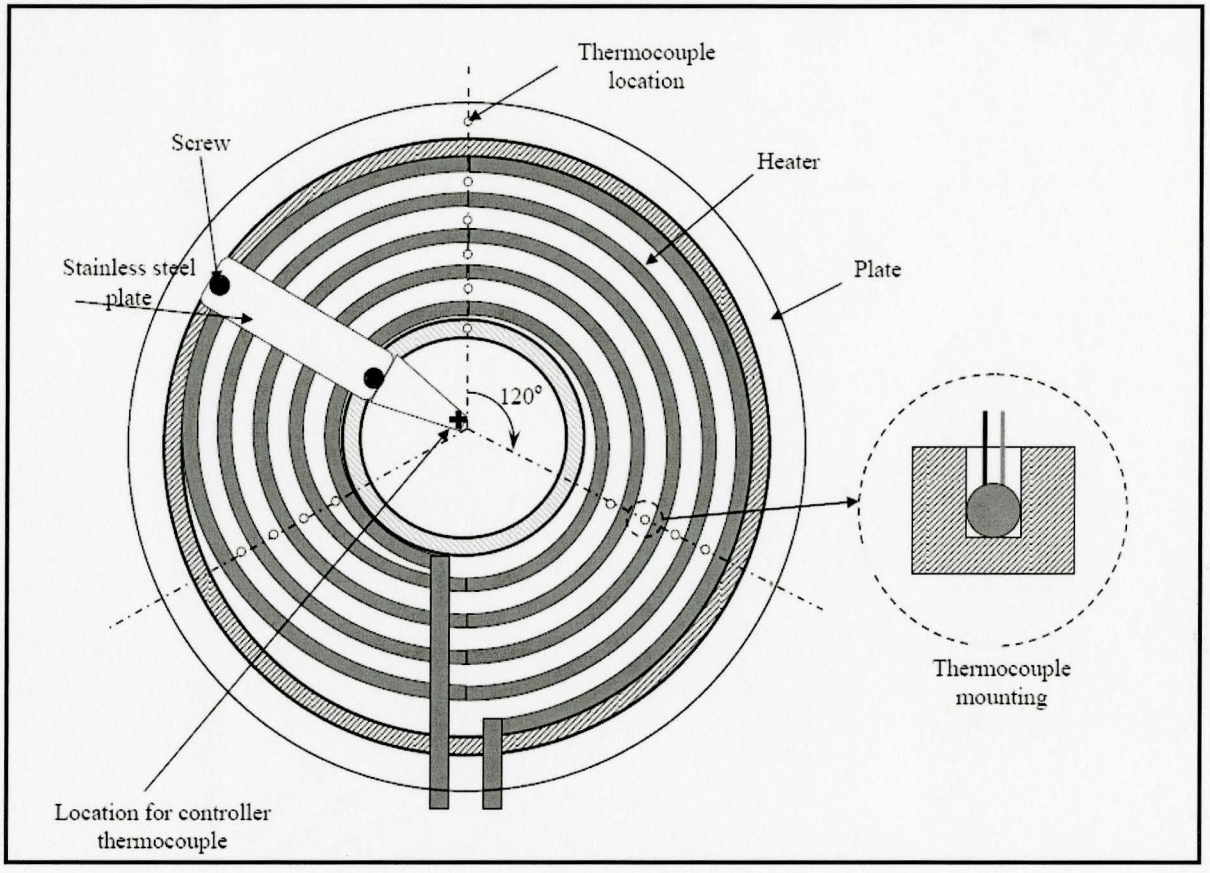

Figure 2.6: Thermocouple Locations.

Figure 2.7 The support plate used to guide the thermocouple wires.

The thermocouples have been carefully mounted in between the heater coil and embedded in the plate to avoid any radiation effects from the heater and to give an accurate representation of the Safe-T Element plate temperature distribution in both the radial and circumferential directions at time intervals of 2 seconds using the FLUKE data acquisition unit shown in Figure 2.3

High temperature thermocouple cement has been tried but it failed because of lack of enough space available for mounting the thermocouple.

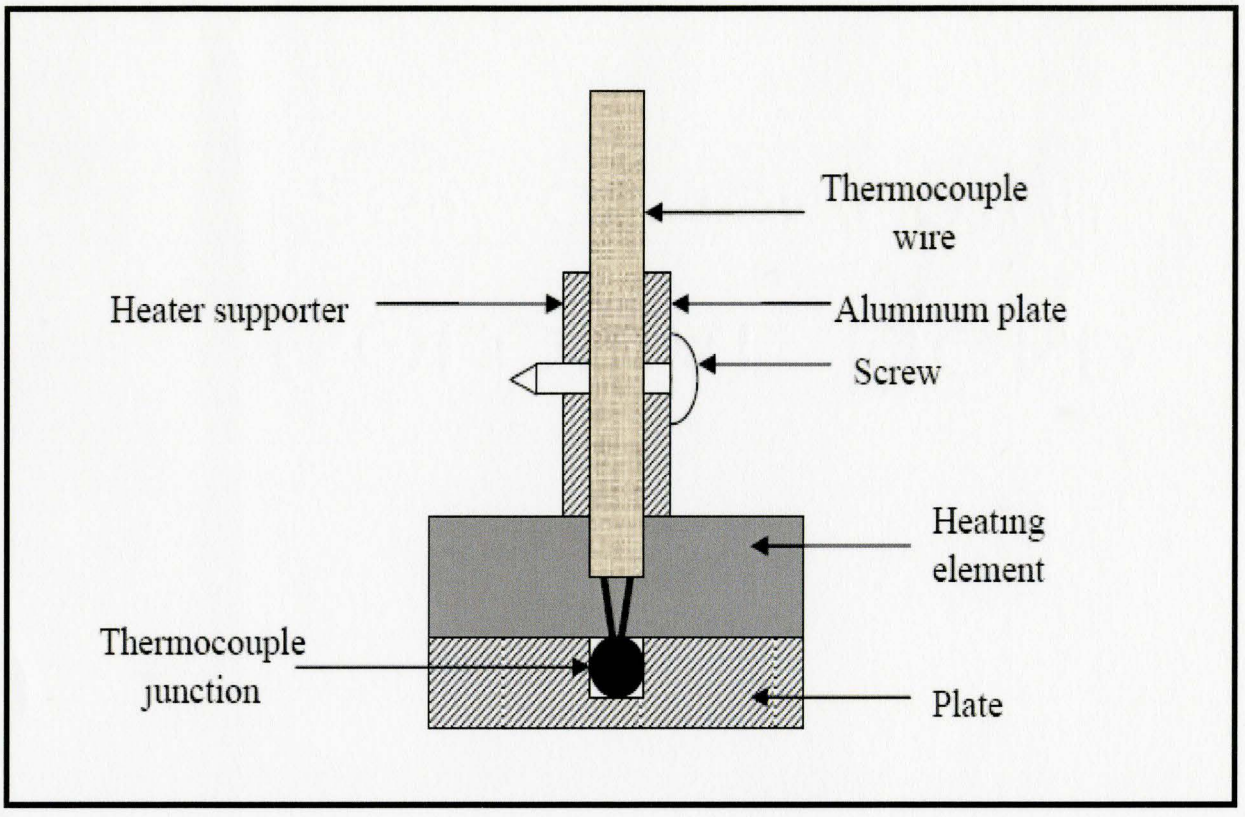

Figure 2.8 Schematic diagram showing the mounting process of the thermocouple

The most beneficial idea that was found to work reasonably well was drilling holes about 2/3 of the plate thickness where the thermocouple bulb can be embedded into these holes and make use of the tri-leg supporter of the heater to fix the thermocouple wire using a small aluminum plate where the wires were sandwiched between the plates and the supporter and screws were used to create the pressure required to fix the wire in place without any movement, as shown in Figure 2.7 and Figure 2.8.

2.4 Deflection Measurement

In order to measure the deflection of the Safe-T Element plate, a special mechanism has been built which has a lever and a pointing tip along with a dial gauge as shown in Figure 2.9

Figure 2.9· Mechanism devised to measure the deflection of the Safe-T Element plate

The dial gauge is very sensitive, so any slight disturbance or looseness in the joints caused a problem in the measurement of the actual deflection. So this method of measuring the deflection was discarded.

For this reason a Filler Gauge (Figure 2.10) has been used to measure the accuracy of the Filler Gauge for the range for 0.04 - 0.15 mm is +/- 0.005 mm and in the range of 0.20 - 0.30 is +/- 0.012 mm. It has been observed that the maximum deflection takes place at the centre of the Safe-T Element plate.

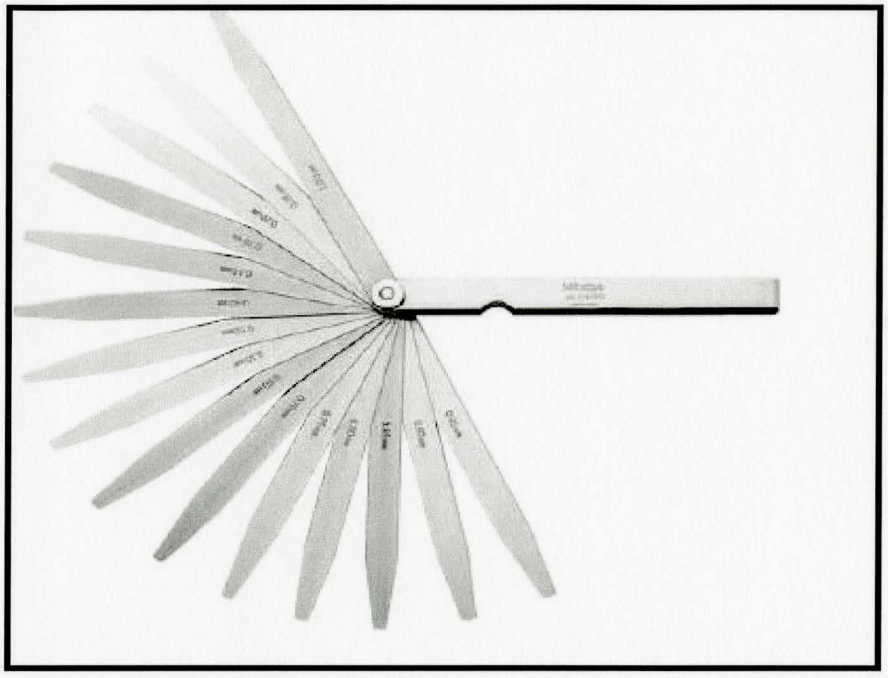

Figure 2.10: Filler gauge used to measure deflection

Chapter 3

3 Experimental Result

3.1 Introduction

One of the challenges that were faced at the beginning of this project is the lack of information provided by PTI about the details of material and grade of Cast Iron used in the manufacturing of the Safe-T Element. Therefore, the chemistry of the Safe-T Element plate had to be investigated to determine the type of material provided to PTI. This has been followed by a tensile test and a study of the microstructure to acquire enough information about the grade and properties of the material.

3.2 Chemical Analysis

The Iron Carbon phase diagram (Figure 3.1) shows the temperature as a function of the weight percentage of carbon. According to this phase diagram, a material is known to be Cast Iron if the weight percentage of carbon at 1148°C lies between 2.11- 4.3 [2]

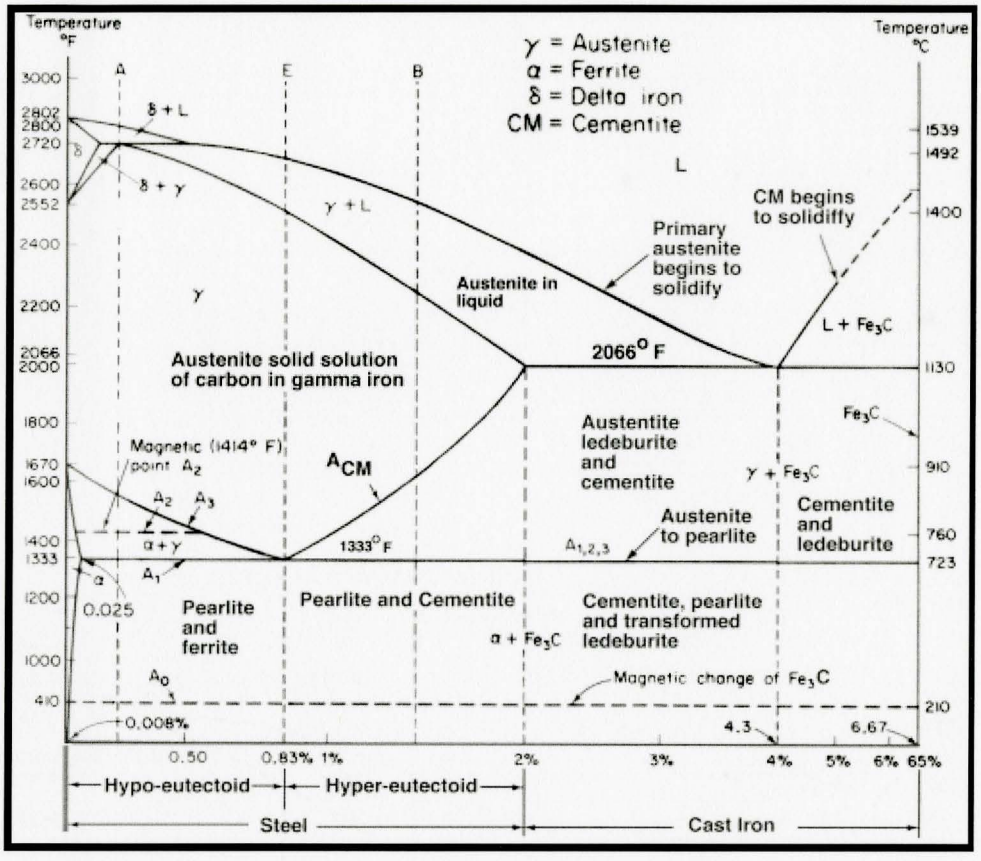

Figure 3 1 Iron Carbon Phase Diagram [10]

Glow Discharge Optical Emission Spectroscopy in the department of Material Science, McMaster University has been used for chemical analysis as shown in Figure 3.2.

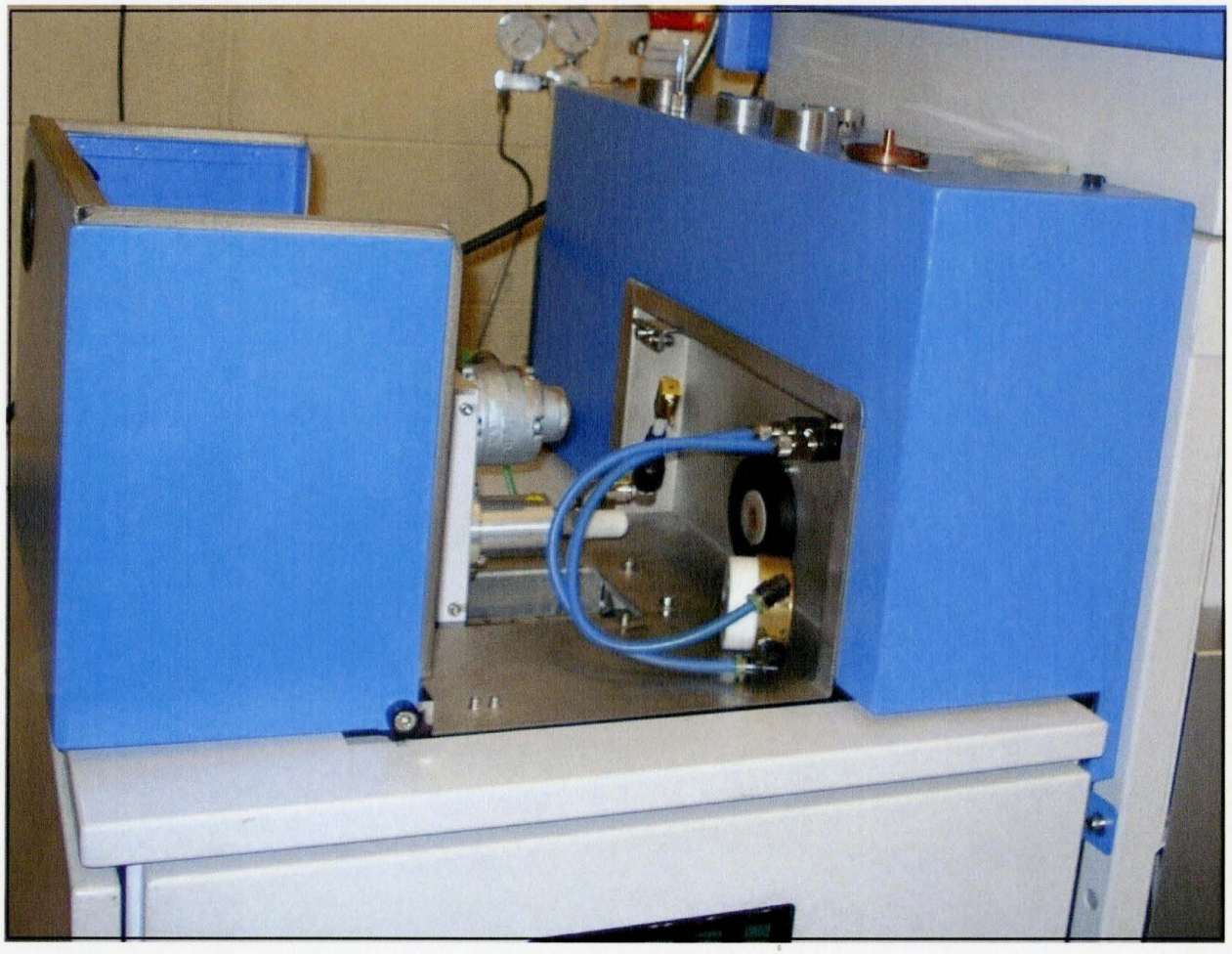

Figure.3.2. Glow Discharge Optical Emission Spectroscopy, Department of Material Science, and McMaster University

Four different measurements of chemical analysis for the same sample made from Safe-T Element plate referred as test1, test2, test3 and test4 has been taken as shown in Table 3 1 An average of these four measurements has been taken as the final value for the chemical analysis test as shown in the result column of the Table 3 1 The weight percentage for carbon has found as 3 1752 from the final averaged result, this weight percent of carbon lies within the range specified for the Cast Iron. The carbon equivalent value is 3.922, which is calculated as CEV = %C + 1/3%Si + 1/3%P, also indicates that material is Grey Cast Iron.

Table 3.1: Results of the Chemical Analysis.

Element	Result	SD	RSD	Test1	Test2	Test3	Test4
C	3.1752	0.00667	0.21	3.1674	3.1719	3.1799	3.1815
P	0.26855	0.000698	0.26	0.26849	0.26791	0.26827	0.26954
S	0.1257	0.00201	1.6	0.1264	0.1234	0.1249	0.1281
Si	1.9711	0.00375	0.19	1.9667	1.9693	1.9738	1.9744
Ti	0.08973	0.000422	0.47	0.0896	0.08927	0.09029	0.08974
Fe	93.22	0.014	0.015	[93.231]	[93.232]	[93.215]	[93.203]
Mg	0.00131	0.000144	11	[0.0012]	[0.00116]	[0.00144]	[0.00142]
Mo	0.06112	0.000141	0.23	0.06096	0.06109	0.06112	0.0613
Al	0	0	0.8	0	0	0	0
Mn	0.3804	0.00316	0.83	0.3814	0.3772	0.3786	0.3843
Cr	0.10926	0.000328	0.3	0.10917	0.10941	0.10961	0.10885
Ni	0.21293	0.000362	0.17	0.21344	0.21281	0.2126	0.21287
Cu	0.2818	0.000395	0.14	0.28125	0.28219	0.28179	0.28196
V	0.102841	0.000095	0.092	0.102789	0.102753	0.102967	0.102856

3.3 Tensile Testing

Tensile testing is a method in which an increasingly tensile load is applied on the specimen Figure 3.3, and the corresponding elongation in the specimen due to this load is then measured. This increasingly load is applied till the point where the specimen breaks into two separate parts. This experiment has been carried out at four different temperatures to determine Young's modulus and the yield strength of the material as a function of temperature. The device used for this test is shown in Figure 3.4.

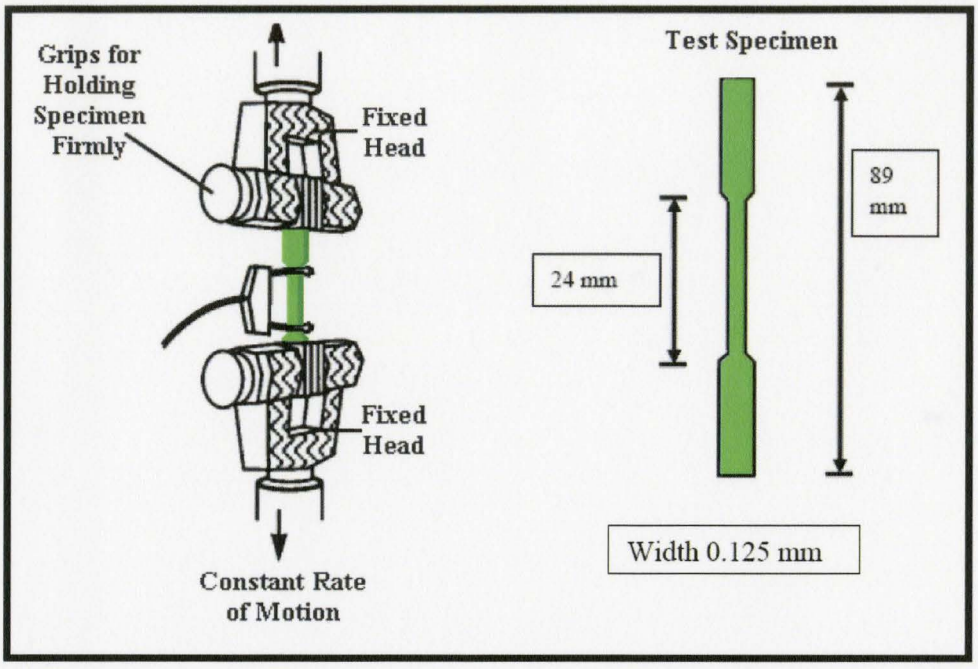

Figure 3.3 Dimension of the specimen used for the tensile test

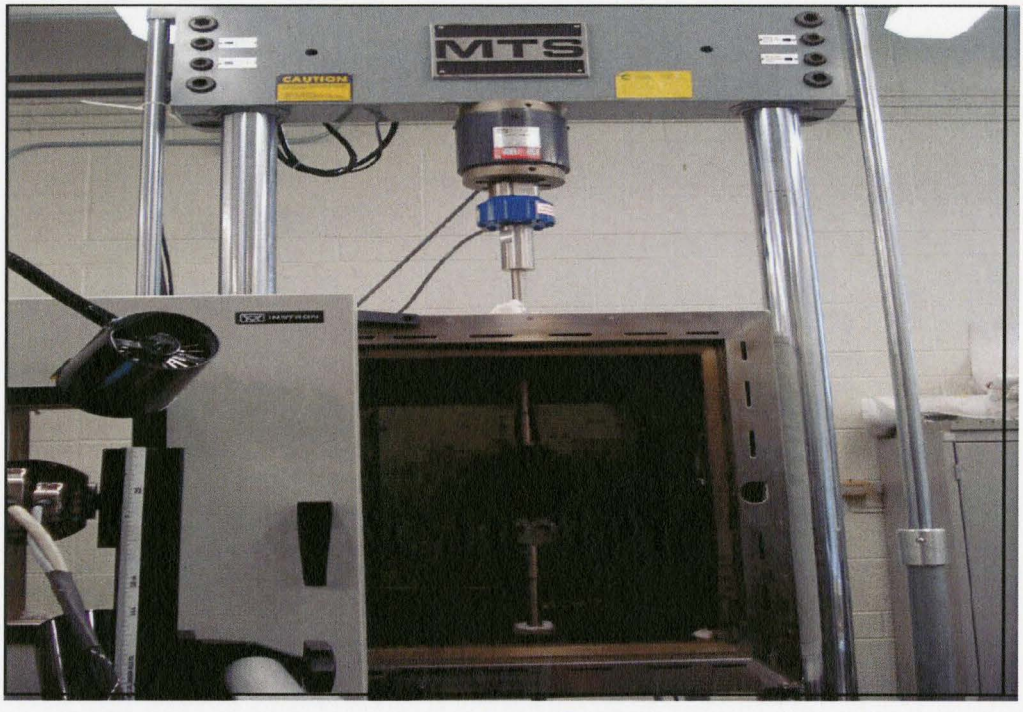

Figure 3.4: Experimental Setup for tensile test

The Gray Cast Iron behaves very differently under tensile loading from other types of Cast Iron mainly because of its microstructure [12] In the Gray Cast Iron, shape of graphite is in the flake form leading to stress concentration resulting in failure at a lower stress than the Ductile Cast Iron as shown in Figure 3.5

Gray Cast Iron is brittle in nature, for this reason ultimate tensile strength is reported for the commercial grading of Gray Cast Iron [21] In order to determine which grade of Cast Iron has been used in the Safe-T Element plate, tensile tests for the sample of the element are required.

Chemical Composition alone is not enough to specify the Grade of Gray Cast Iron used for the Safe-T Element plate. According to ASTM (American Society for Testing Material), Gray Cast Iron has been classified into class 20 to 60 depending on the minimum tensile strength [5]

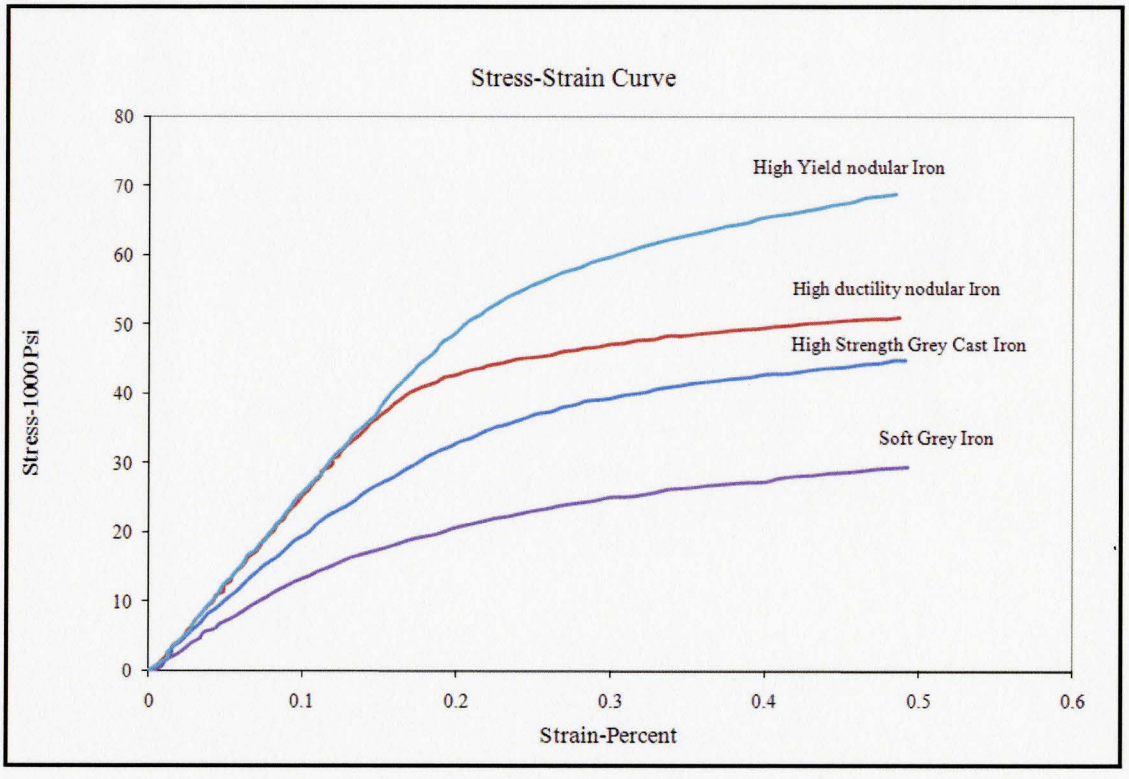

Figure 3.5 Typical Stress-strain curves for various types of Cast Iron [2]

The minimum tensile strength is also required to determine the grade of the Safe-T Element material. For example, class 20 of Gray Cast Iron has a minimum tensile strength of 20,000 psi.

Specimens were prepared for the tensile test according to ASTM E8-87a standard, with the dimension indicated in the Figure.3.3 A gradually increasing tensile load is applied on the specimen and the corresponding increase in the length of the specimen is measured and recorded until the specimen is broken. This test has been carried out at different temperatures to draw the stress - strain curve of the specified grade of Cast Iron used. Five samples were tested. The results of the tensile test are plotted in Figure 3.6. As shown, at 23°C and 100 °C, specimen does not show any variation with initial applied stress. For 200 °C and 300 °C, initial data for variation between the stress and strain is not available. The specimen at 300 °C shows less stress than 200 °C, which could be due to error in the way experiment has been carried out.

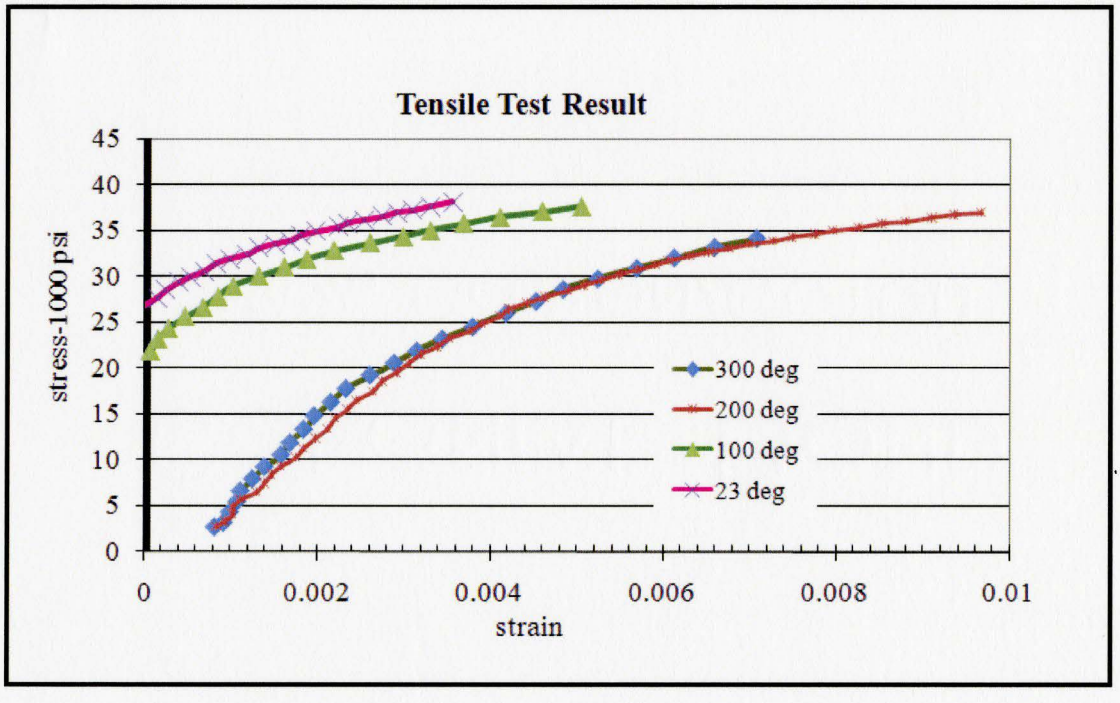

Figure 3.6: Experimental results of the tensile tests

3.4 Testing the uniformity of the Microstructure of Safe-T element Plate Material

The microstructure of Gray Cast Iron has mainly two main parts, metal matrix and the graphite flakes. In order to identify the metal matrix and the graphite shape, samples have been prepared and polished with very fine abrasive and later viewed with a high-resolution Lecia Optical Microscope shown in Figure3 7

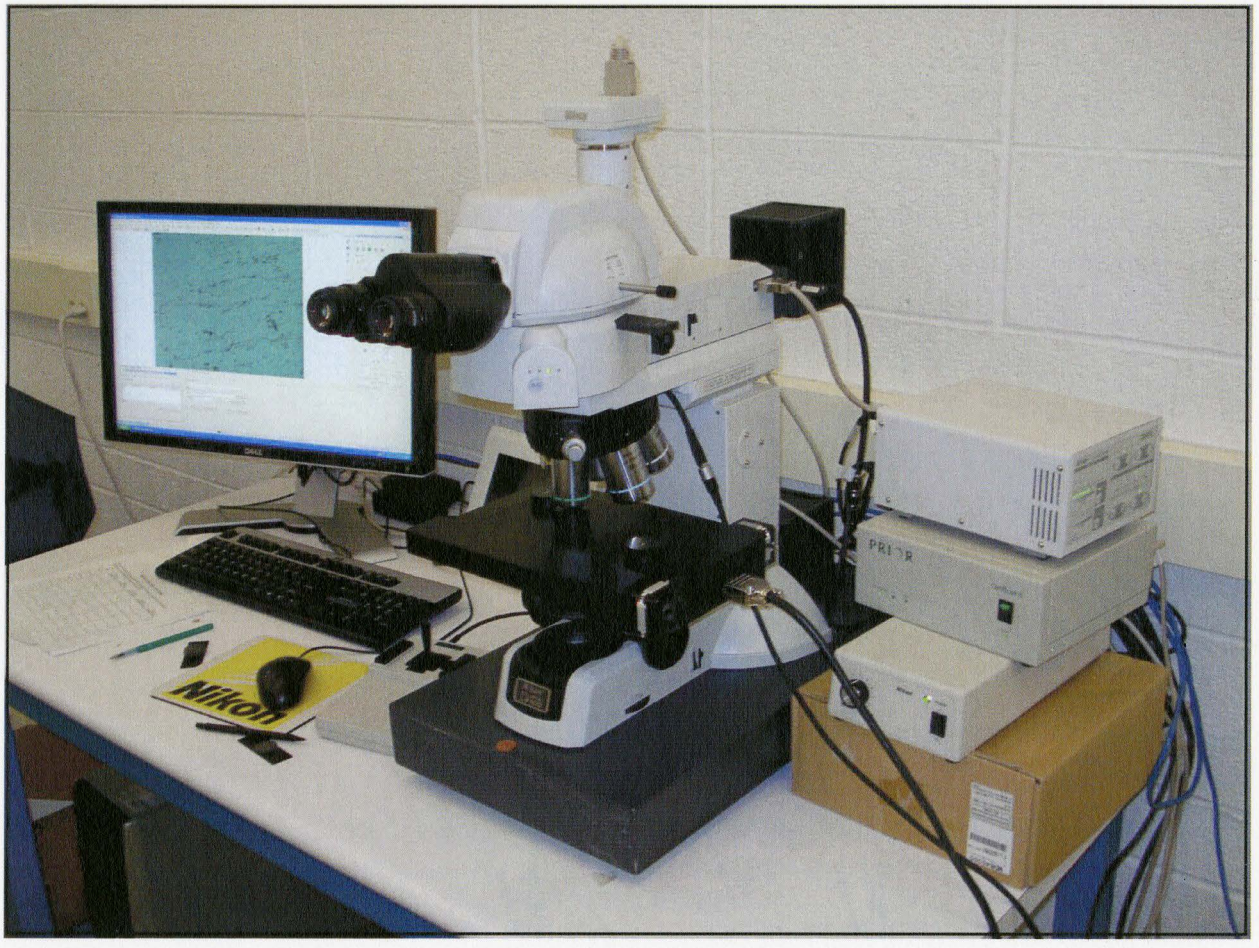

Figure 3 7 The Leica Optical Microscope.

To establish the type of graphite and its distribution, a sample is first photographed in unetched condition. After this, by etching the polished surface of the sample with the nital acid, the matrix structure could be observed. Formation of different types of microstructure of Gray cast Iron has already been discussed in detail in chapter 1

The matrix of the Gray Iron could be all ferrite or all pearlite as shown in the Figure 3.8, or a mixture of these constituents. The ferrite is carbon free, but could have other material as solid solutions. The tensile strength for ferrite is low, but this type of metal matrix provides excellent machinibilty The tendency to form ferrite increases with the presence of graphitizers and by increasing the carbon equivalence. At the same time an increase in the carbide stabilizers and a faster cooling rate of casting reduces or eliminates the amount of free ferrite in the matrix. Pearlite consists of alternate plate of soft ferrite and iron carbide, which is hard in nature. Due to formation of pearlite in the metal matrix, the strength of Gray Cast Iron increases. This metal matrix can be changed by heat treatment, but graphite shape does not change after being formed during the casting process.

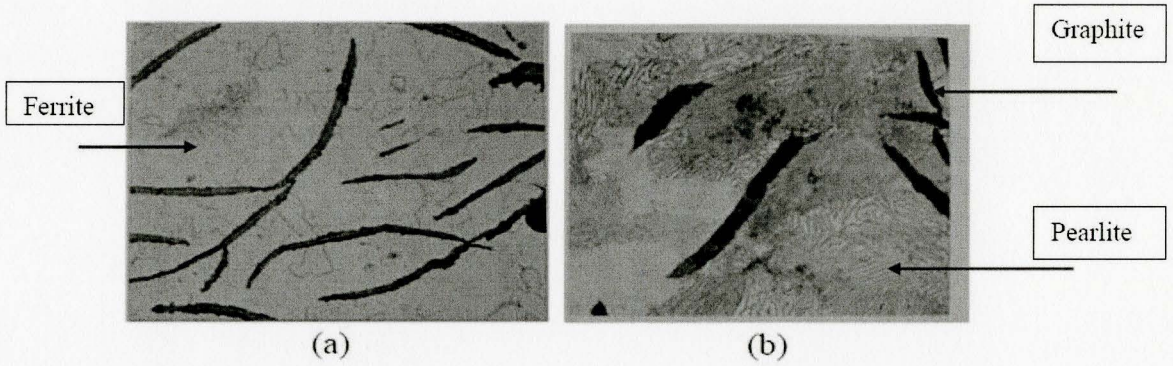

Figure 3.8: (a) Gray Cast Iron with a ferritic matrix at 250X magnification, Figure 3.8 (b) Gray Cast Iron with a pearlitic matrix at 500X magnification [2]

It can be observed from the result of the microstructure investigation carried out in this work, shown in Figure 3.9, that the material of the Safe-T Element plate is homogenous and uniform. The graphite is present in the flake form, and the matrix surrounding the graphite flakes is ferrite. The microstructure shown in Figure 3.9 is uniform, which indicated the deformation of the Safe-T Element plate is not due to microstructure non-uniformity

Figure 3.9· Microstructure of the Safe-T Element material at 160X

3.5 Testing the stability of the Safe-T Element plate Material

Differential Scanning Caleromitry (DSC) is a technique to measure the energy necessary to establish an almost zero temperature difference between specimen of a substance and an inert material. These two specimens are subjected to identical temperatures in an environment heated or cooled at a controlled rate. This test is carried out to test the release of energy from the sample, which gives an indication of the thermal stability of the material.

DSC test has been carried out using the DSC unit 2910 model shown in Figure 3 10.

Figure 3 10: The DSC unit.

In a DSC test there are two pans. One pan is called the reference pan having, which may or may not have standard weights, this pan remains empty during the present test. In the other pan has material from Safe-T Element plate has been kept. The sample required for the DSC test should have 2-10 mg weight. Each pan is electrically heated at a specific rate, usually in the range of 10-20°C per minute.

Having extra material in the sample pan means that the sample pan would require more heat to keep the temperature of the sample pan increasing at the same rate as the reference pan. This requires extra heat is what is measured in the DSC experiment. Experiments were carried on two

samples made from the Safe-T Element plate from the two different suppliers, referred to here as supplier-P and supplier-C.

Three runs were carried out during the DSC test for each sample as shown in Figures 3 11 and 3 12. The results from the DSC test indicate that the material of Safe-T Element plate is thermally stable as there is not much difference in the energy required between the consecutive second and third runs for both the samples. In the first run there was a substantial greater amount of energy absorbed by the sample, which could be affect of heating on the microstructure in the very first cycle of heating in the DSC test.

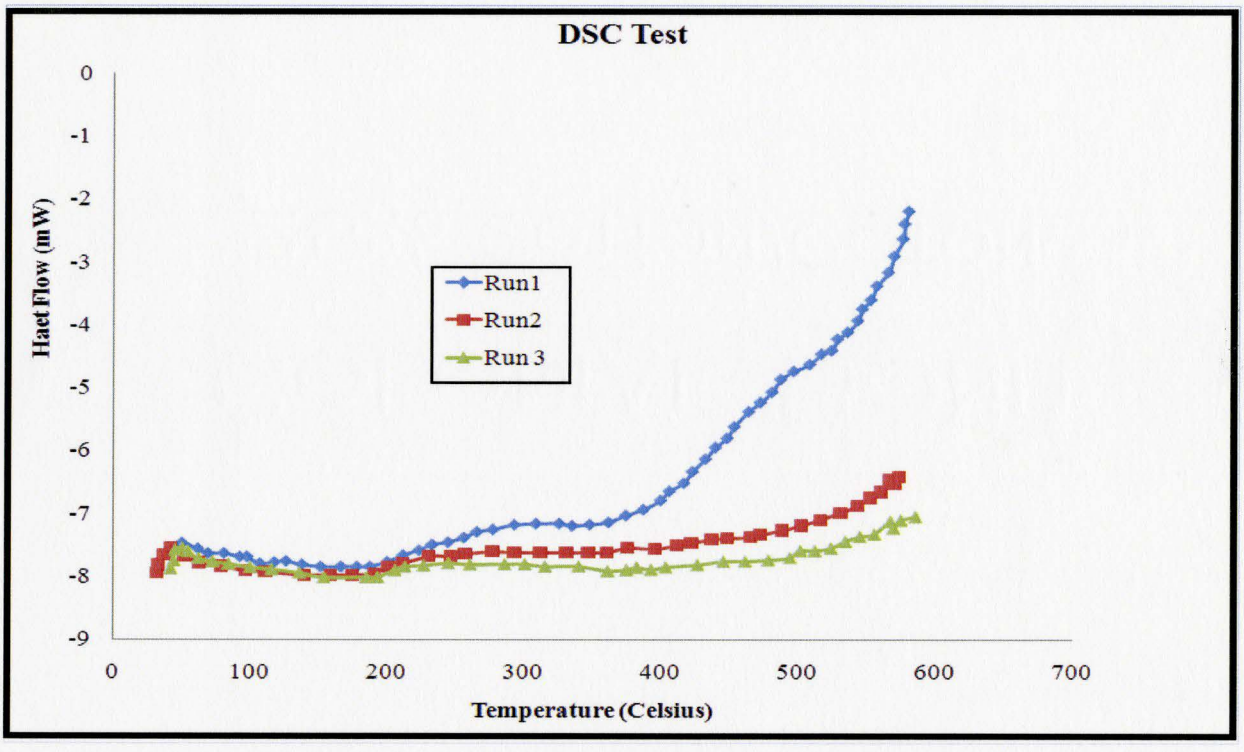

Figure 3 11 Results of the DSC test for a sample made of Gray Cast Iron plate from supplier-P

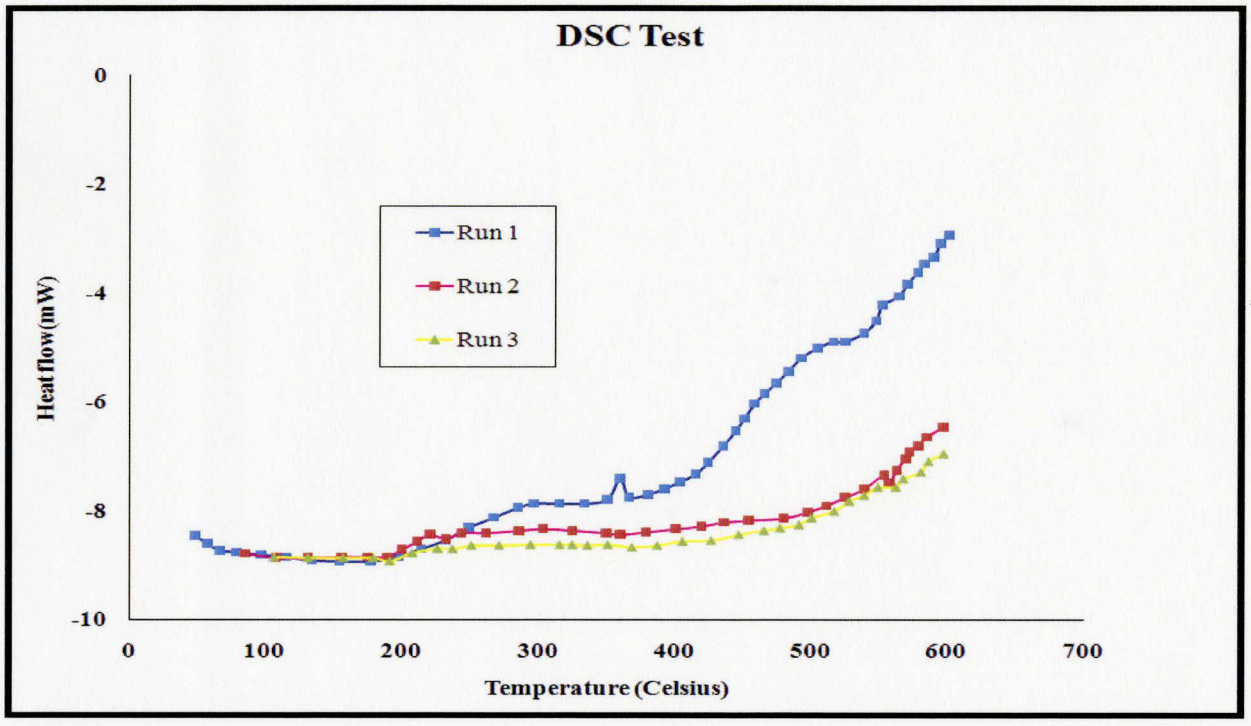

Figure 3 12. Results of the DSC test for a sample made of Gray Cast Iron plate from supplier-C

3.6 Testing the Effect of Residual Stresses in the Safe-T Element plate

The Safe-T Element plate is cast from Gray Cast Iron, which is followed by machining, shot peening and finally enamelling.

Internal stresses are expected to be present in the plate due to any uneven cooling during the casting and due to the shot peening process. If untreated, any unbalanced internal stresses could be the cause of the deformation problem of the Safe-T Element plate. Therefore, a set of experiments was performed to examine the possibility of internal stresses as a cause of the deformation of the plate.

A Safe-T Element plate was repeatedly heated on the stove in the range of 500-550°C for more than 100 times. It was observed that the plate comes to their original shape after the cooling. Repeated heating did not permanently distort the Safe-T Element plate; and the

therefore the possibility of internal stresses as possible cause for the distortion of the Safe-T Element was ignored and this was concluded that the there is thermal buckling of the plate.

3.7 Effect of Thermal Cycling

The nature of the use of the Safe-T Element plates exposes it to thermal cycling, it was necessary to observe the influence of thermal cycling on the plate performance. For this purpose, a plate was exposed to a typical heating for more than 100 times and the temperature has been measured in each time and the plate deflection was observed. Table 3.2 and Figure 3 13 show the number of thermocouples and their locations on the plate.

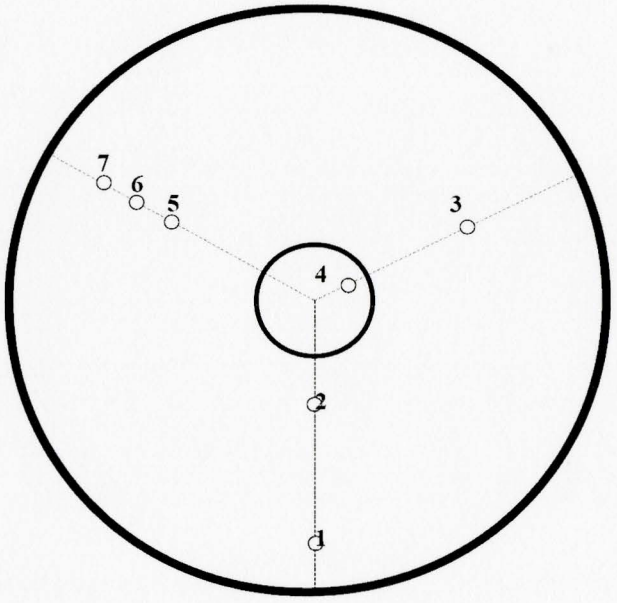

Figure 3 13 Schematic diagram of the Safe-T Element plate, showing locations of the thermocouples used during the thermal cycling test.

Table 3.2: Locations of thermocouples shown in Figure 3.15.

Thermocouple No	Radius(mm)	Angle (Θ)
1	85.66	0
2	70.82	0
3	42.70	120
4	15.03	120
5	58.03	240
6	71.00	240
7	86.51	240

The results of these experiments are shown in Figure 3.16

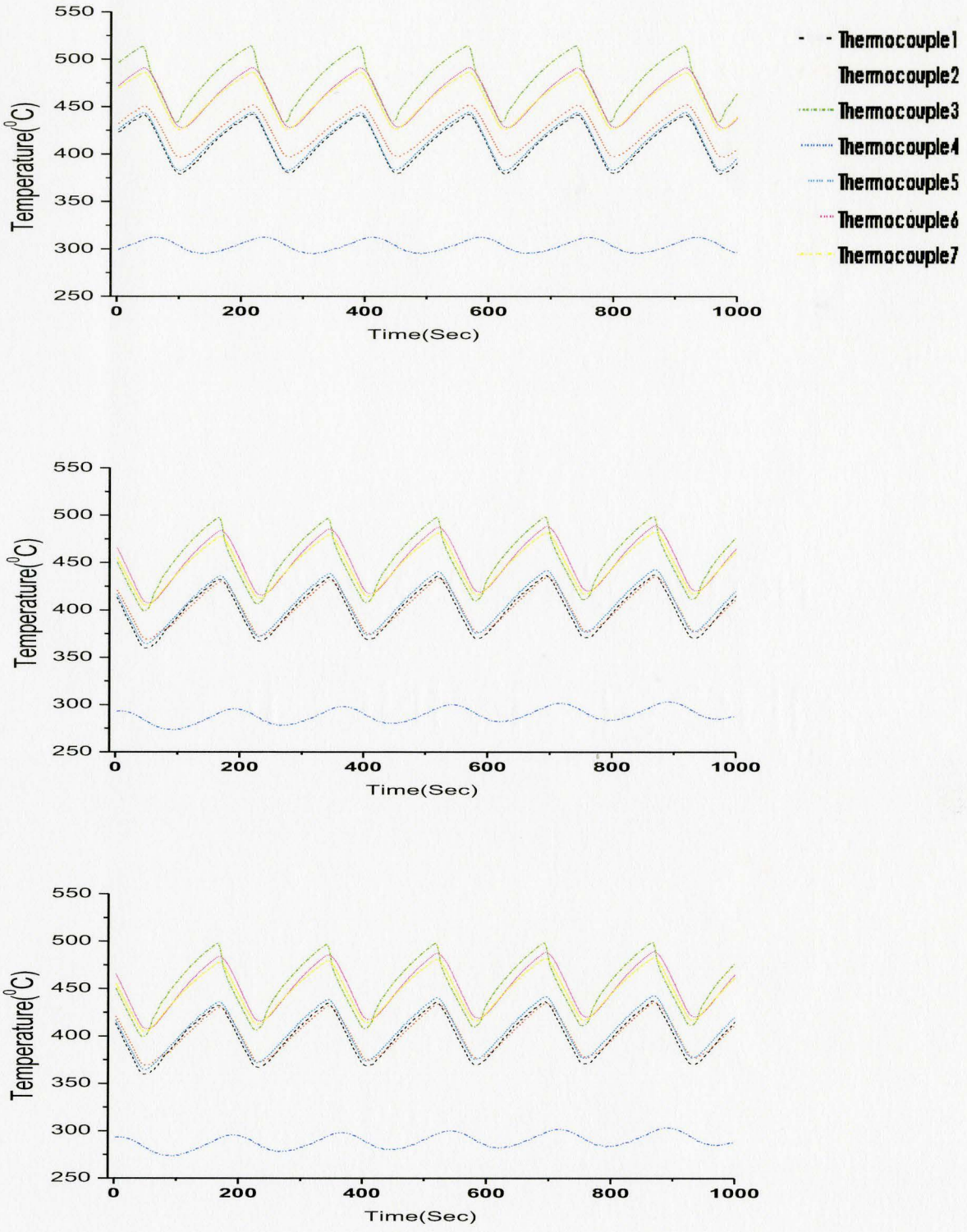

Figure 3 14: Temperature profiles measured with seven thermocouples during the thermal cycling tests.

Thermal cycling test were carried out with the temperature controller set at 400°C. Results of these tests are shown in Figures 3.15 and 3.16. Other tests were carried out without any limit on the maximum temperature. So, in these tests the maximum temperature was dependent on the maximum capacity of the heating element. Results of these tests are shown in Figures 3.17 and 3.18.

The deformation of the Safe-T Element plate was observed during these thermal cycling tests. Same value of deformation was observed during the different heating cycle of the same plate, which ruled out the possibility of internal stresses as the root cause of the distortion of the plate. Result of the thermal cycling test made us to believe that the root cause of the deformation problem is thermal buckling due to non-uniform heating of the Safe-T Element plate.

The effect of heat transfer between the top and bottom surface of the plate has been neglected based on the value of Biot number. The value of Biot number comes less than 0.1 and calculated as hL/K, where h is convective heat transfer coefficient of air, L is the thickness of the plate taken as 3.5 mm and value of K for the plate has been taken as 46.020 (w/m-K). A thermal cycling test was also performed by making large groove in the bracket (Stainless steel clip (Figure 1.2) to secure radiant heating element) allowing free movement of plate in the radial direction. This test showed the same of value of deformation as without the groove in the bracket.

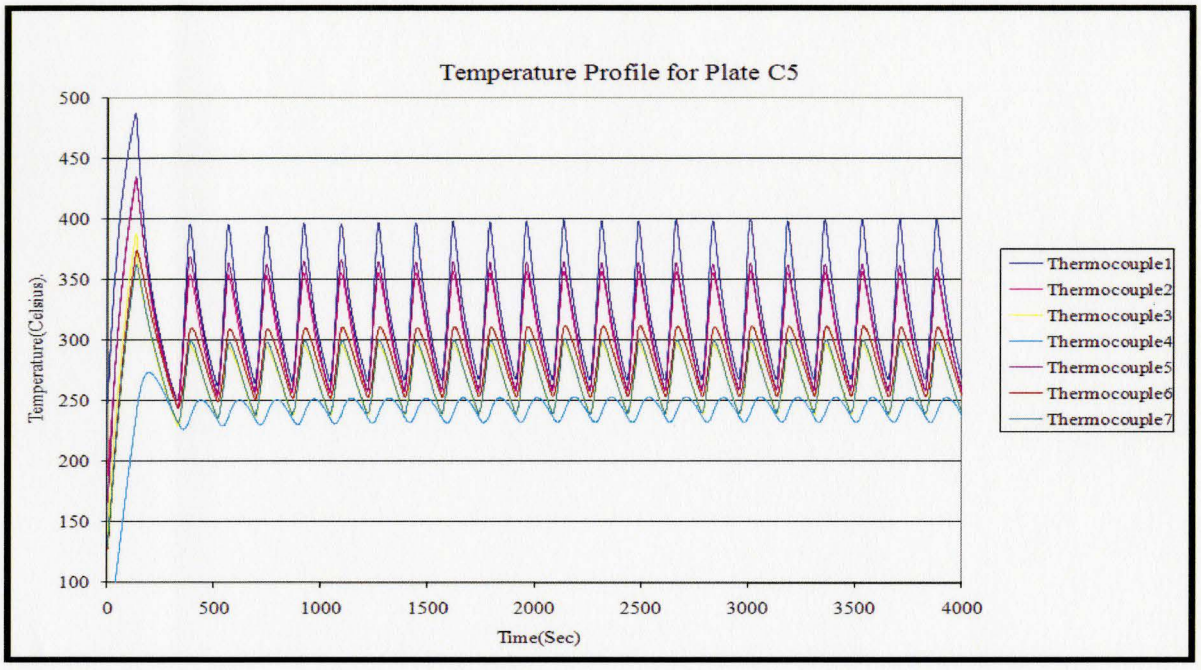

Figure 3 15 Thermal profile for a Safe-T Element plate from supplier C at Controller temperature = 400 °C.

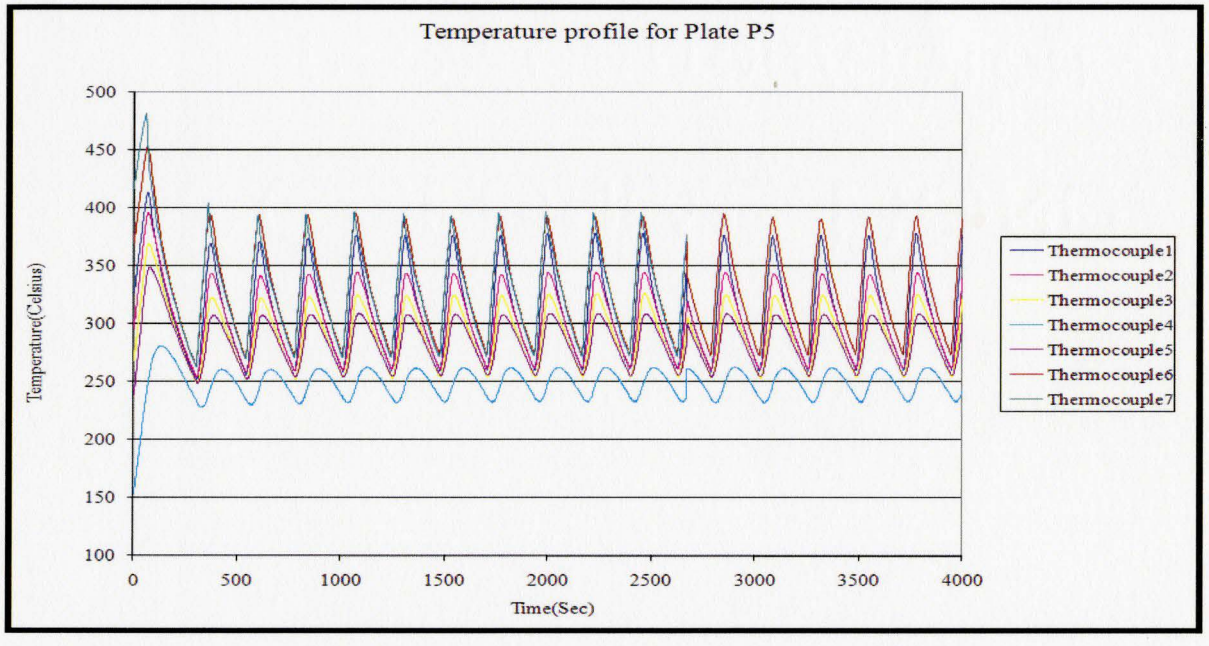

Figure 3 16: Thermal profile for a Safe-T Element plate from supplier P at Controller temperature = 400 °C.

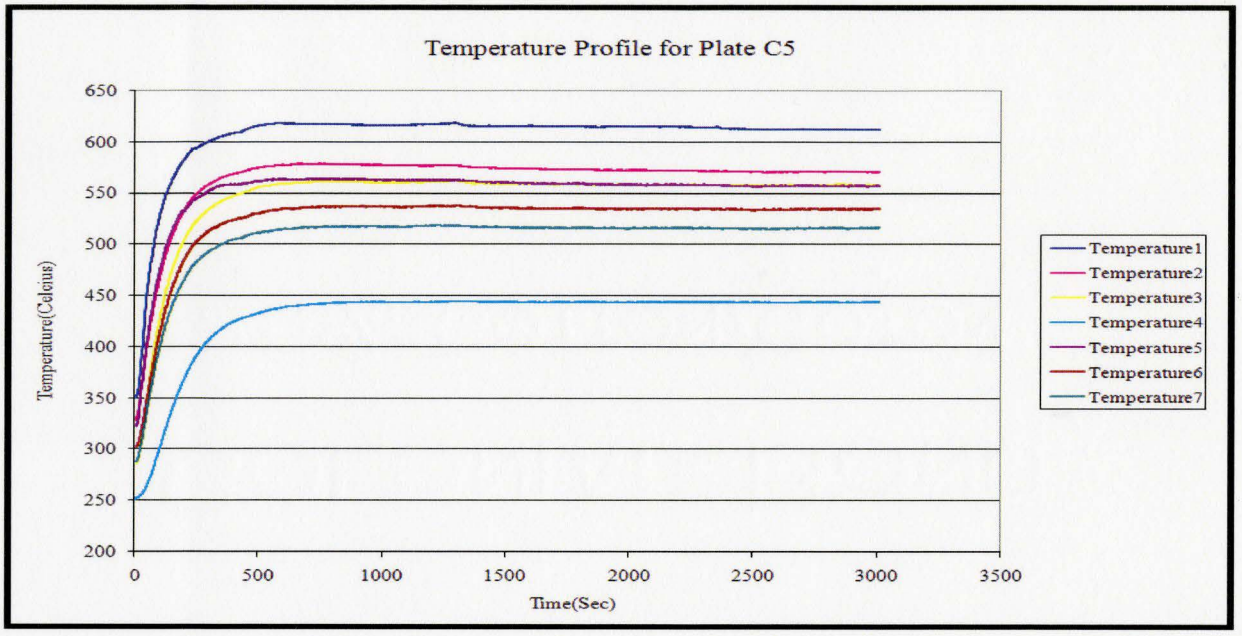

Figure 3 17 Thermal profile for plate C5 Test was carried out with the maximum heating capacity of the heating element.

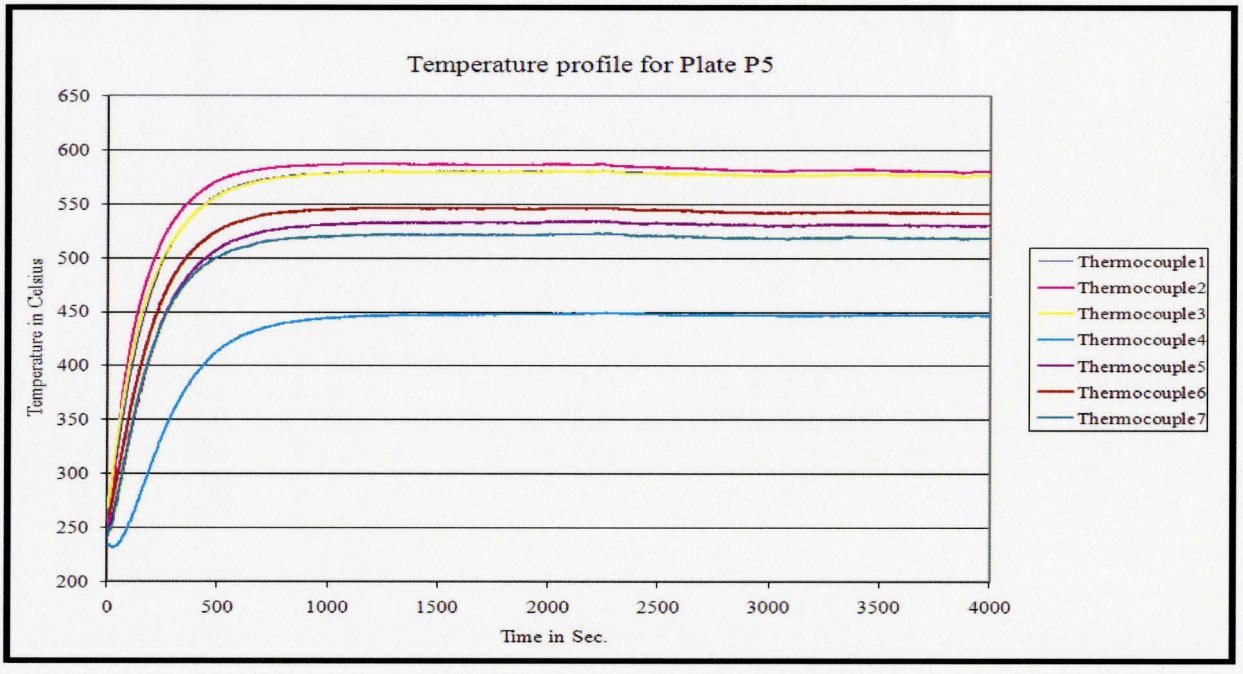

Figure 3 18. Thermal profile for plate P5 Test was carried out with the maximum heating capacity of the heating element.

3.8 Temperature Uniformity Tests

The number of thermocouples has been increased. This was done in order to get a better understanding of the temperature variation across the three support plates of the heating coil. The number of thermocouples has been increased to 12 to observe the temperature variation in the radial and circumferential direction as shown in Figure 3.19.

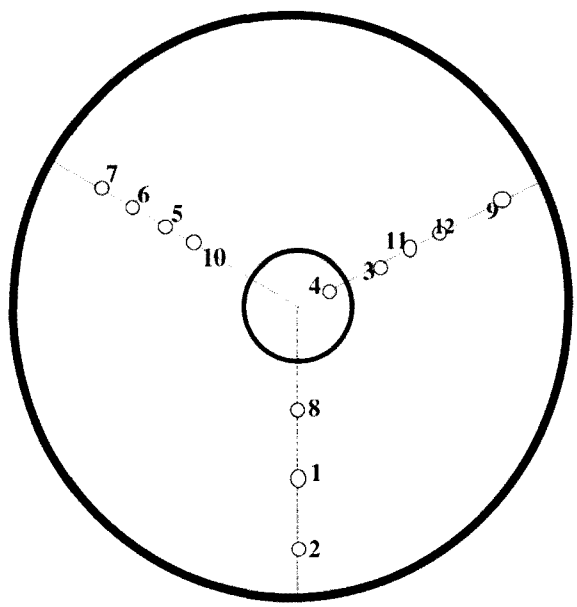

Figure 3.19: Locations of the 12 thermocouples mounted on the Safe-T Element plate used during the uniformity tests.

Table 3.3 shows the locations of the thermocouples shown in Figure 3.19. For the purpose of consistency the locations of the previous 7 thermocouples as shown in Figure 3.13 have been kept the same. Figures 3.20 and 3.21 show sample of the temperature profile recorded by using 12 thermocouples shown in Figure 3.19.

Table 3.3 Location of thermocouples

Thermocouple No	Radius(mm)	Angle (Θ)
1	70.82	0
2	85.66	0
3	42.70	120
4	15.03	120
5	58.03	240
6	71.00	240
7	86.51	240
8	42.60	0
9	84.00	120
10	46.55	240
11	56.38	120
12	70.46	120

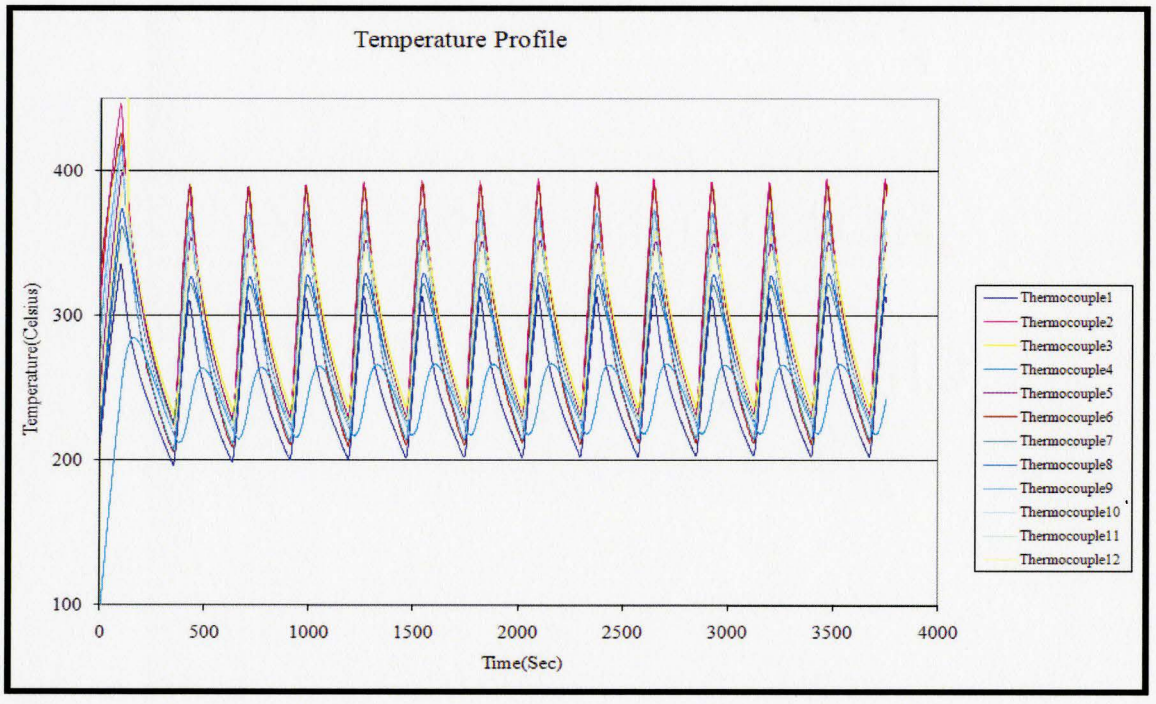

Figure 3.20: Temperature profiles measured during a uniformity test with controller set at 400°C.

The recorded temperature distribution as function of time and location is shown in Figure 3.23 for a controller set temperature of 400°C. As shown, the temperature distribution reaches steady state after about 1200 s, i.e., 20 min. After that the temperature variation with time becomes repeatable. It is worth noting, from this figure, that the difference between the controller temperature and the maximum temperature of the Safe-T Element plate, reaches about 125°C.

This difference is caused by the location of the controller thermocouple which is mounted on the stainless steel (SS) plate that fixes the heater to the Safe-T Element plate. The SS Plate is in direct contact with the heating element not with the Safe-T Element plate. Therefore, most of the heat conducted through the SS plate is coming from the heater which is at a higher temperature than that of the Safe-T Element plate.

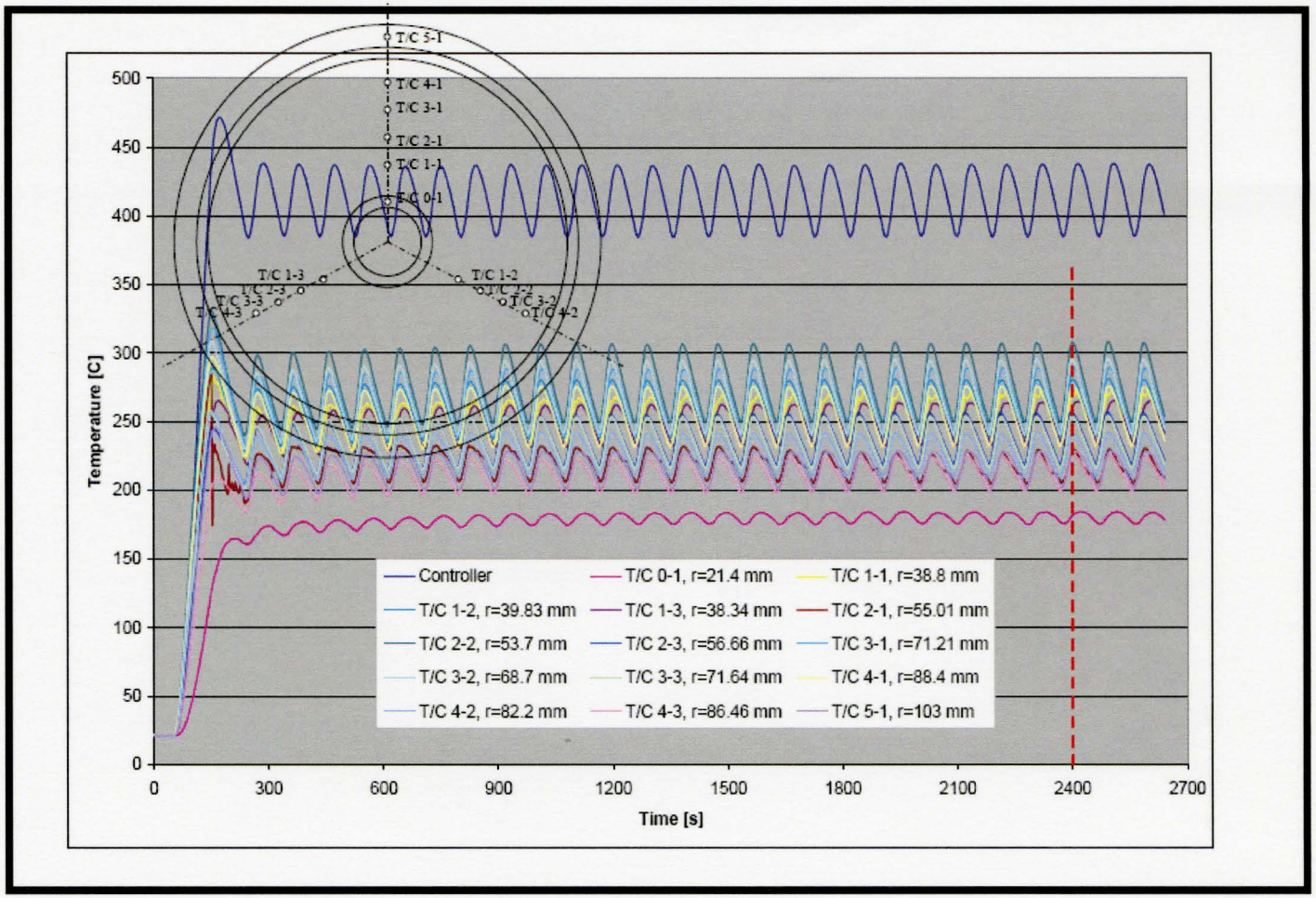

Figure 3.21 Temperature profiles measured during a uniformity test with controller set at 400ºC.

Figure 3.24 shows the averaged temperature variation from the circumferential and radial directions as function of the radius of the plate. This averaged temperature Profile was generated after fitting the data (temperature variation as a function of time) collected from Figure 3.21 at time 2400 sec and fitting the data using a fourth order polynomial.

The fourth order polynomial used for fitting the data is

$$T = 1E - 06\, r^4 + 0.00\, r^3 - 0.18\, r^2 + 1.65E + 14.53\, r \quad 50.76$$

It can be observed from Figure 3.24 that the maximum temperature takes place at r = 52.93 mm, almost half the plate radius.

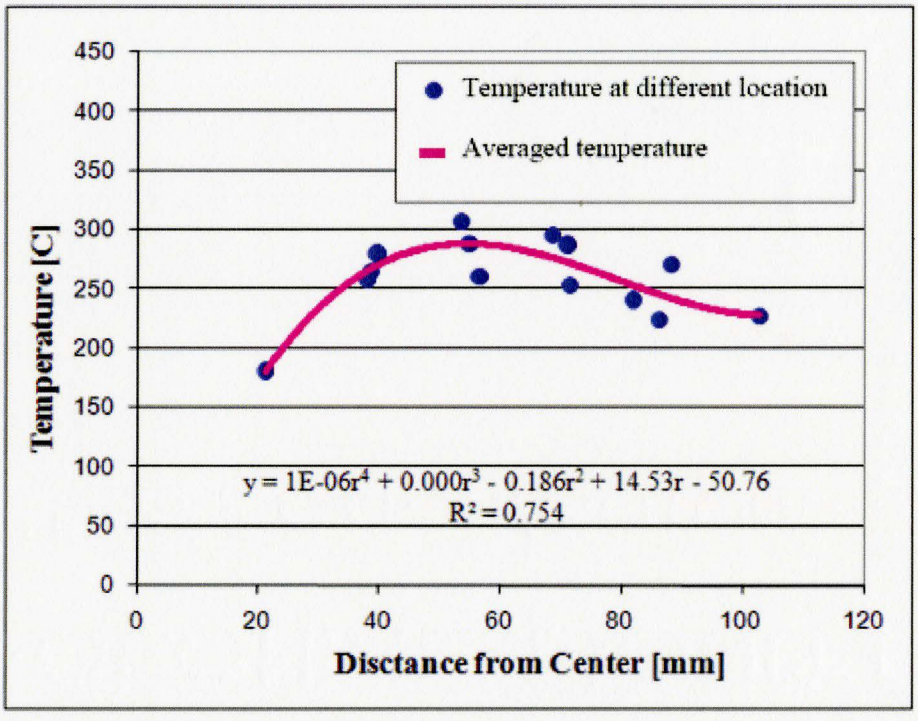

Figure 3.22. Averaged temperature distribution as function of the plate radius. This distribution has been determined using data shown in Figure 3.21

3.9 Deflection Measurement

The maximum deflections for the Plates have been measured using a filler gauge at the maximum temperature of the plate and found to be 0.35 mm difference between the centre and the edge of the plate. It has been observed from the experiment that the maximum deflection is almost half at plate radius and decreases gradually on both sides in the radial direction. The maximum allowable deflection set by PTI is 0.1 mm.

Chapter 4

4 Numerical Investigation

4.1 Introduction

In order to study the effect of the geometrical parameters and the material properties on the deflection of the Safe-T Element plate, a numerical investigation has been performed using the finite element software package LS-DYNA. In order to determine the maximum deflection of the plate (the worst condition), the radial temperature profile at the time of maximum temperature (Figure 3.22) has been used as a boundary condition in the numerical simulations. A fourth-order polynomial fitting of this profile is shown in Figure 4.1 applied on the Safe-T Element plate. As shown, the maximum temperature on the plate takes place at a distance of about 52.93 mm from the centre of the plate.

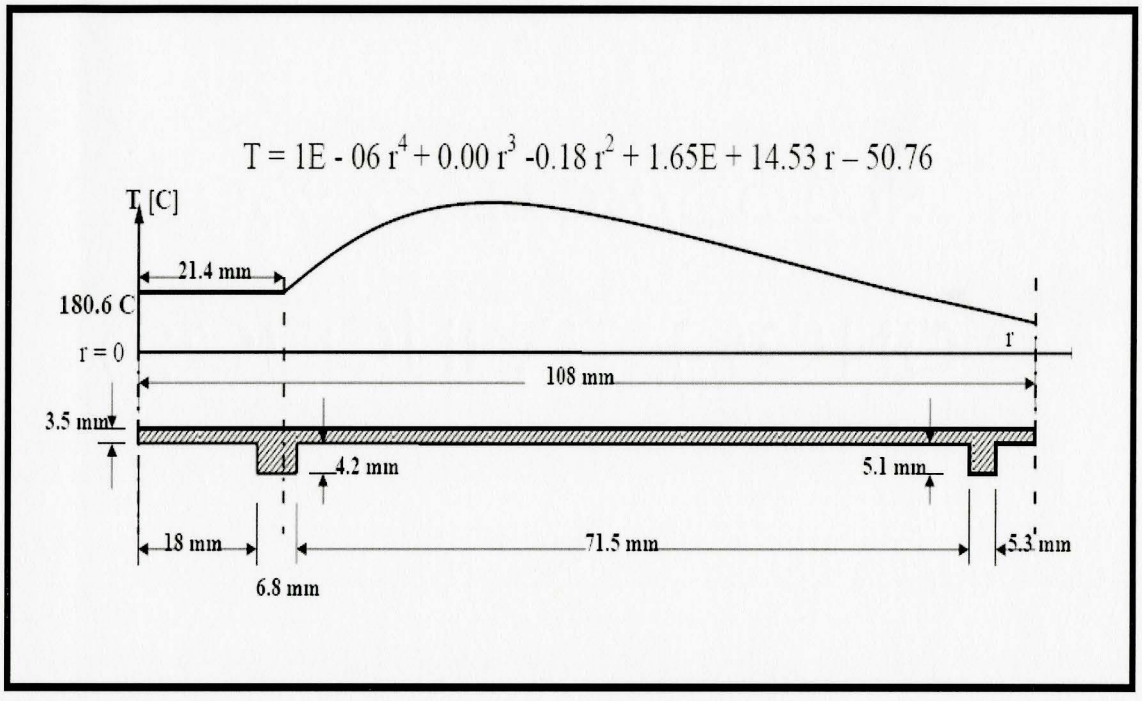

Figure 4.1 Side view of the Safe-T Element plate, showing the temperature profile as function of the plate radius.

4.2 Procedure of the Numerical Investigation

The Numerical Investigation of the Safe-T Element plate has been carried out in the following steps.

1 Two- dimensional (2D) simulations of the simplified geometry without any rings attached to the plate (Figure 4.1). For this simplified geometry, the effect of each individual material property on the plate deflection has been investigated.

2. 2D simulations of the real geometry with rings have been performed and the numerical result of the deflection has been compared with the experimental results.
3. Simulations have been carried out of the real geometry to investigate the effect of the plate thickness on the deflection.
4. Simulations of some modifications of the current geometry to minimize plate deflection have been carried out.

4.3 Material Properties used for the Numerical Investigation

According to the microstructure analysis and the results of the tensile test, it has been found that the closest class of Cast Iron to the Safe-T Element plate material is class 40. Therefore, material properties of class 40 of Gray Cast Iron as function of temperature have been used in the numerical investigation. These properties have been obtained from the available literature [2] and from software packages like EDU Pack [22] and MPDB software [23]. The result of the tensile test has been used to determine the value of young's modulus and the yield strength as a function of the temperature. The values of various material properties such as the coefficient of thermal expansion, yield strength, young's modulus and Poison's ratio are shown in Table 4.1. The value of the thermal conductivity and the heat capacity of class 40 have been taken as 46.020 (w/m-K) and 450.00 (J/ (Kg-K)) from the EDU Pack Software [22]. The value of Poisson's ratio has been taken as 0.3 [22].

Table 4.1: The values of the mechanical and thermal properties of class 40 of Gray Cast Iron used in numerical investigation

Temperature (°C)	Yield Strength (N/mm²)	Young's Modulus (N/mm²)	Coefficient of thermal expansion [24] (1/K)
21	263.301	33035.77	.11010E-4
149	256.056	24000.84	.11602E-4
260	248.64	22000.94	.12124E-4
427	177.95	18253.16	.12908E-4

4.4 Numerical Simulations of the simplified geometry (without rings).

The Safe-T Element plate is symmetrical in shape and therefore a 2D model has been used. In order to study the effect of the material properties on the deflection of the element, the actual geometry has been simplified to a flat plate (disc), without the two supporting rings at the bottom which hold the heating element in place. The rectangular mesh shown in Figures 4.2 has been used.

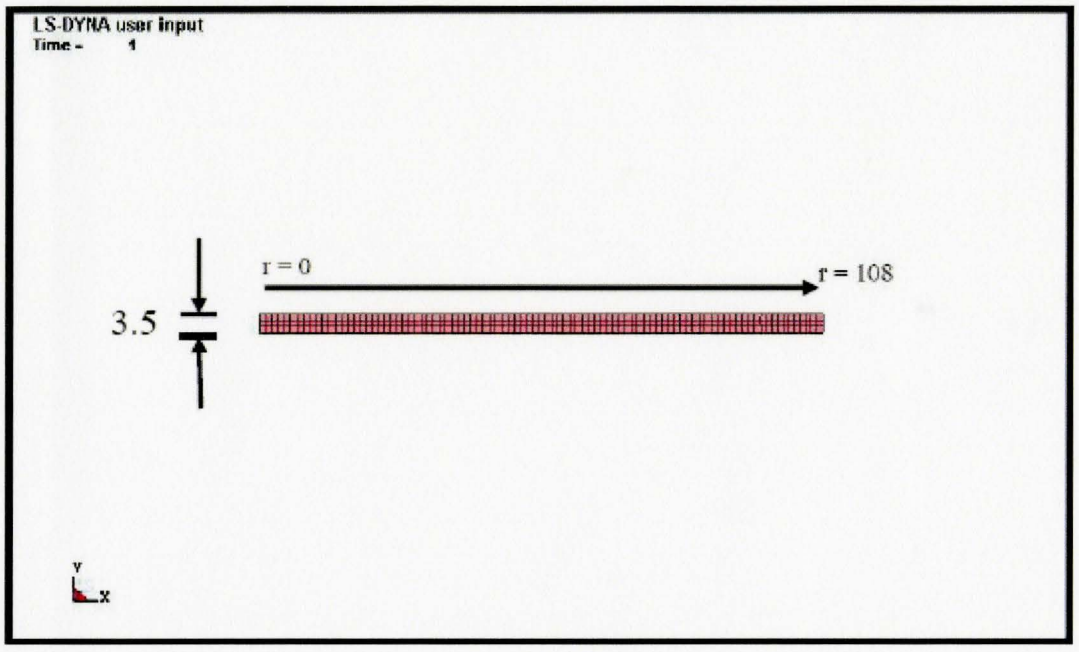

Figure 4.2. Mesh used for the case of the simplified geometry of the Safe-T Element Plate.

Results of this case also allow for investigating the effect of the rings on the deflection of the Safe-T Element after comparing it with the actual case (with rings) as it will be discussed later

The Safe-T Element plate has been divided into 15 separate sets of elements in the radial direction. Shell type of element has been used in the simulation for all these 15 separate sets. A thickness of 1mm has been assigned to each shell type element. Thermal loading has been done by setting an average temperature of each set of consecutive elements from centre to edge of the plate, as shown in Figure 4.3

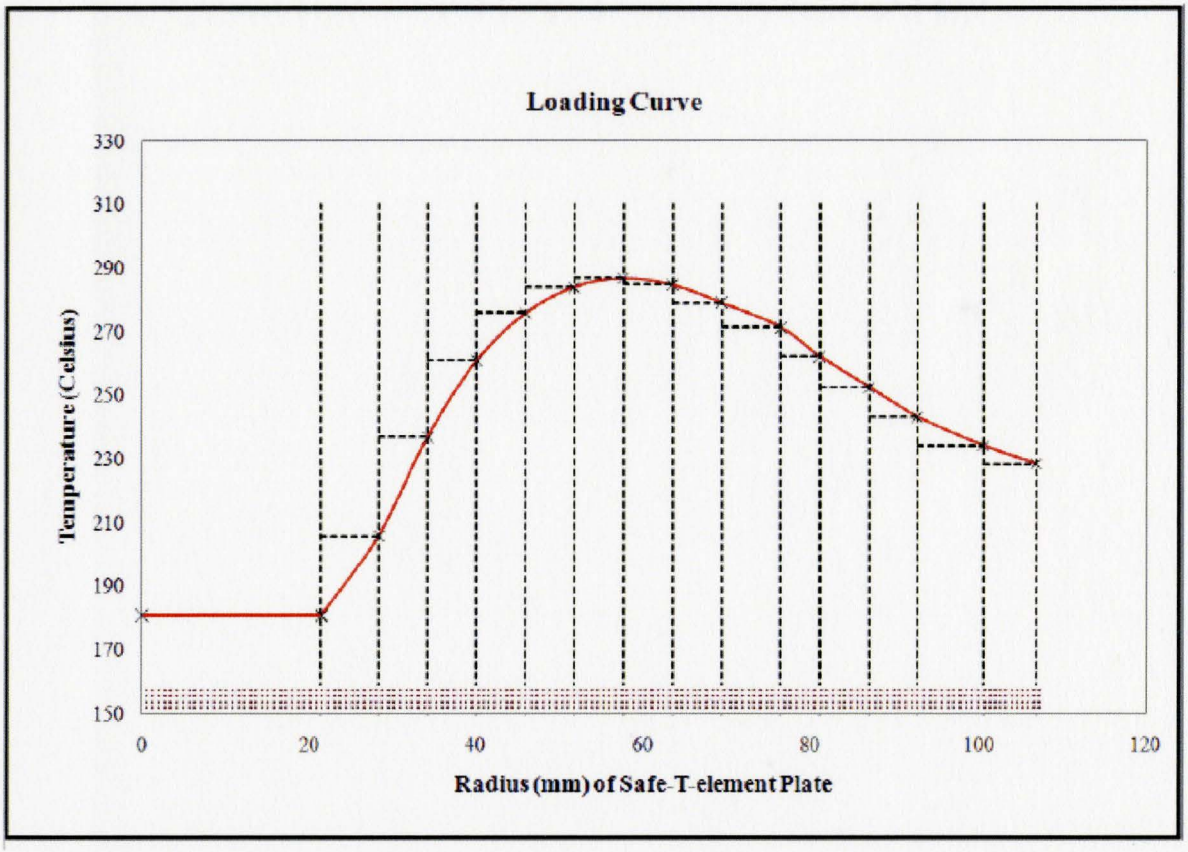

Figure 4.3 Averaged temperature profile used in the numerical simulations

For example at a radius of 20.26 mm the temperature is 180.60°C, so the set of elements in between the centre and r = 20.26 mm has a temperature = 180.60°C and all the elements within this set have the same temperature.

This procedure has been repeated for each set of element. The results of the numerical simulation are shown in Figure 4.4. The value of the effective deflection calculated from this figure is 0.01108073 mm. This effective deflection is the difference between the maximum and the minimum deflections taking place at nodes 569 and 245, respectively,

at a distance of 52.93 mm from the centre of the simplified geometry of the plate. The result of simulation under predicted the value for deflection from experimental result, which is 0.35 mm. Possible reason could be absence of rings attached and the material property used for numerical investigation is of class 40 also assumption has been made while averaging the temperature profile in radial direction.

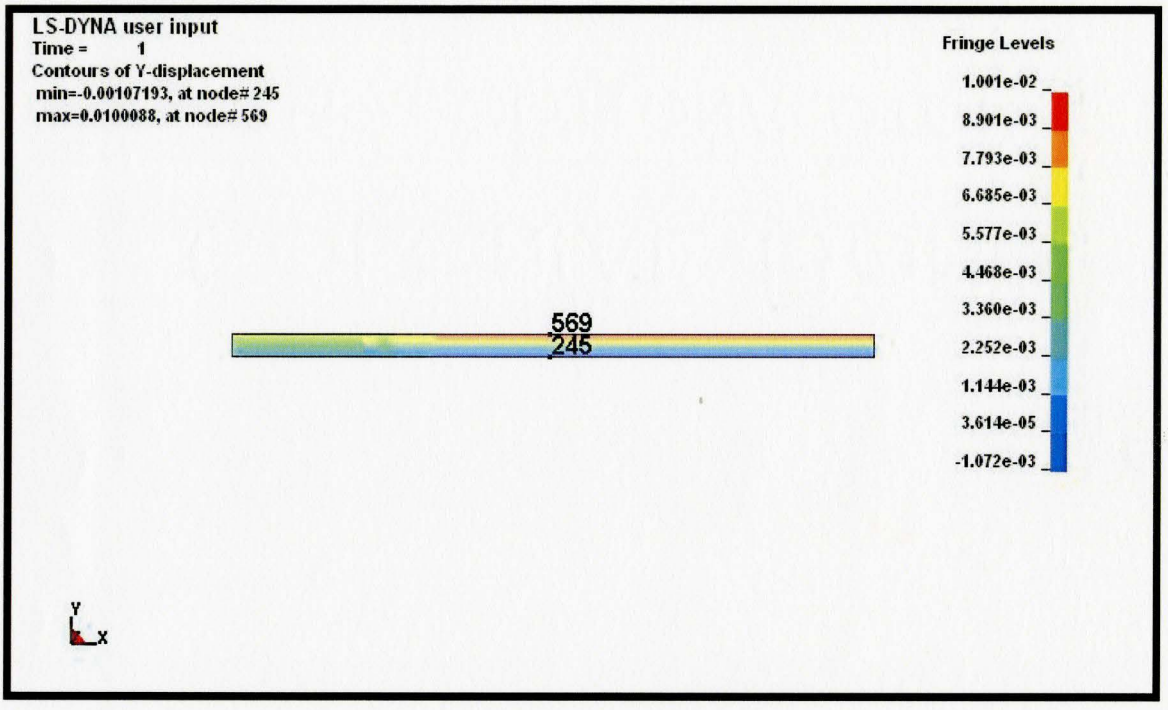

Figure 4.4: Contour plot for the deflection in millimeter along the radius of the Safe-T Element plate. Results obtained by using material properties as a function of temperature listed in Table 4.1

4.5 Simulation of the Actual (current) design of the Safe-T Element plate

A total of 663 nodes have been used to simulate the current design of the plate, as shown in Figure 4.5. A set of 417, 2D shell elements was used. Four nodes were used for each element. The thickness of each element was 1 mm. Initial time step was 0.01 sec to and the software was allowed to select the value of the proper time step of further iterations.

The thermal boundary condition is same as for simplified geometry. The elements on the centre of the plate has been allowed to move in Y direction and free to rotate around X and Z direction. The elements on the perimeter of the plate has been allowed to move in X and Z direction and free to rotate in all three direction. The elements between centre and perimeter of the plate are allowed to move into all three direction of the plate. Temperature distribution within the plate is shown in Figure 4.6. Material thermal properties used as a function of temperature are those listed in Table 4.1.

The simulations of the current design showed an effective deflection of 0.114985 mm. The value of the effective deflection of the simplified geometry is 0.011081 mm which is 90.36 % less than the value of the current design. The location of the maximum deflection of the current design is at the centre of the plate, as shown in Figure 4.7, while in the case of the simplified geometry it takes place at r = 52.94 mm, as shown in Figure 4.4. These results indicate that the two rings in the current design have a significant effect on the maximum deflection. The simulation under predicts the value from the experimental observation which is 0.35 mm. This could be due to uncertainty in the value

of material property and the assumptions taken while averaging the applied temperature profile in the radial direction from the experimental result.

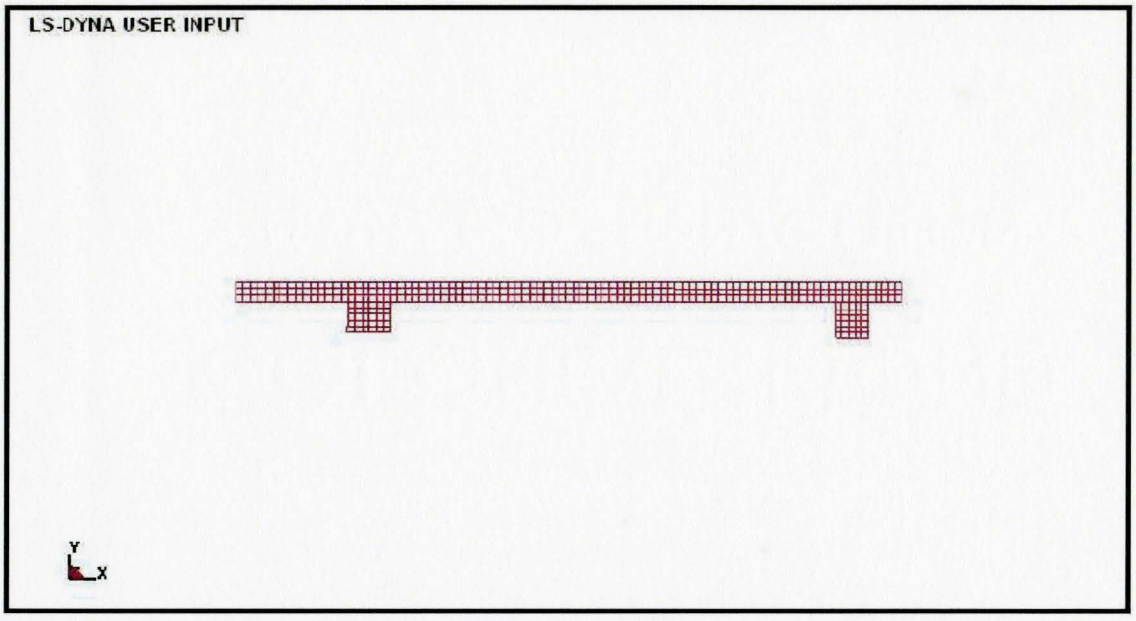

Figure 4.5 Mesh used for the current design.

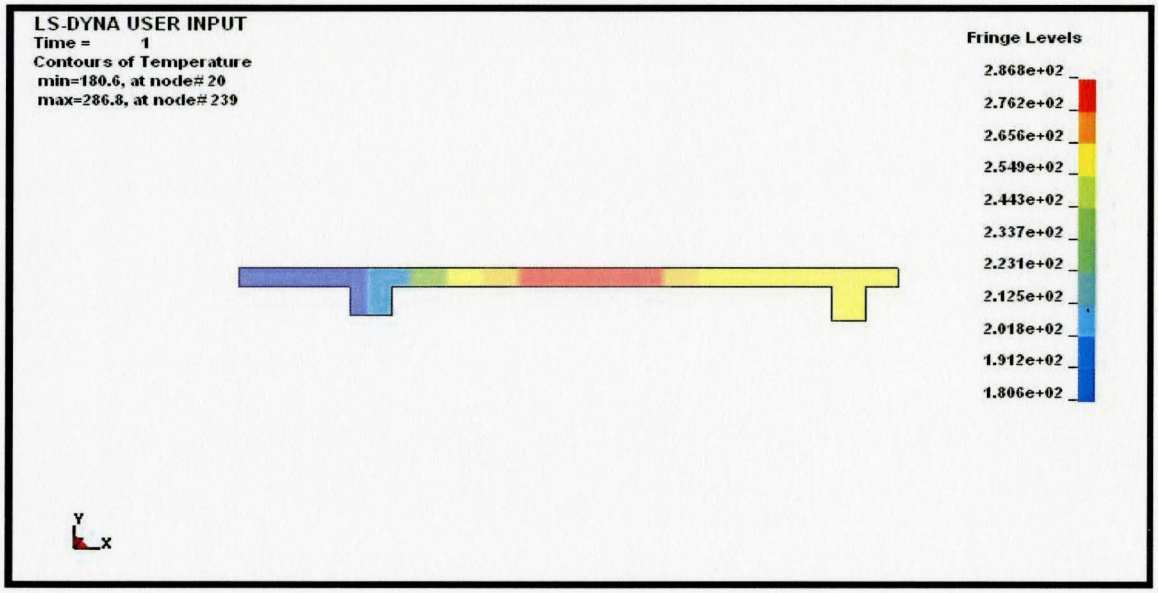

Figure 4.6: Predicted temperature distribution in the current design.

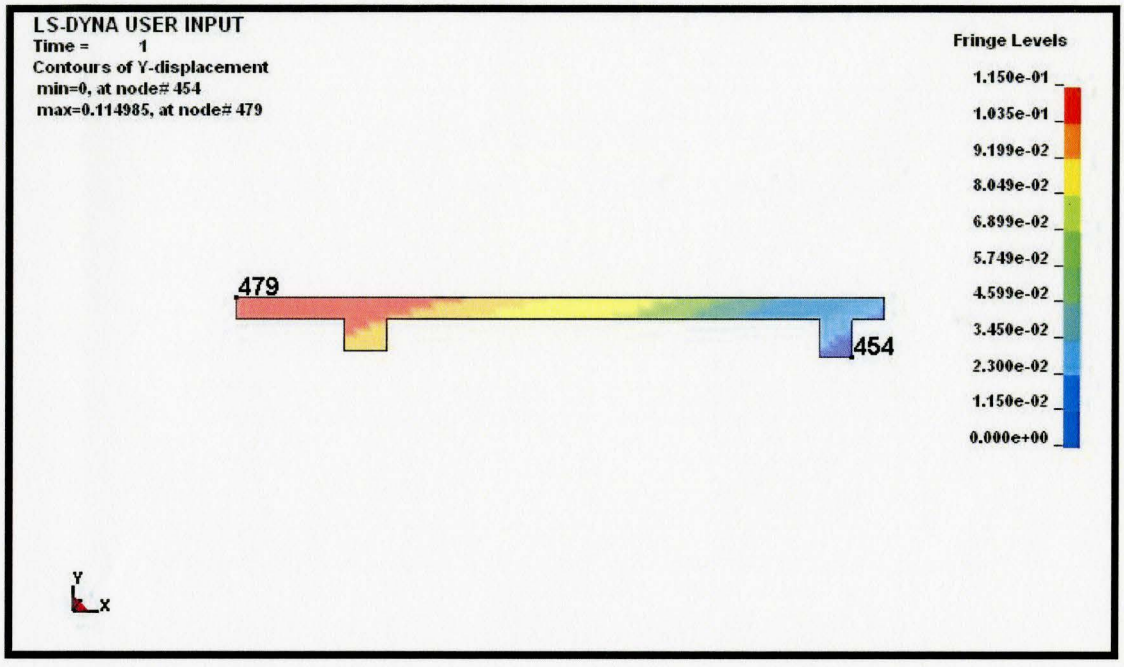

Figure 4.7 Deflection distribution of the current design.

4.6 Effect of material properties on the overall deflection of the simplified geometry.

The numerical results are expected to depend on various material properties such as coefficient of thermal expansion, yield strength, Young's modulus, Poison's ratio, heat capacity and thermal conductivity In order to understand the effect of each individual property on the overall deflection of the Safe-T Element plate, various simulations were carried out by changing only one material property and keeping the value of all other properties unchanged. The results are shown in Table 4.3.All other parameters such as the number of nodes, number of sets of elements and the temperature profile have been kept

the same in all the simulations. Effect of individual property has been discussed separately in the different section:-

4.6.1 Coefficient of thermal expansion

To check the effect of coefficient of thermal expansion on the plate deflection, its value has been increased by 100% from the original value. Due to this effective deflection increases to 0.024414 mm from 0.011081 mm, which is 120.32% more from the old value of the plate. The results of simulation are very sensitive to the value of coefficient of thermal expansion. Table 4.2 the value of the coefficient of thermal expansion of class 40 and a Gray Cast Iron material having chemical composition of 3C-2Si-1Cr-0.7Mn. This can be observed from the Table 4.2 that there is a large difference between the values at higher temperature for class 40 and the material having chemical composition of 3C-2Si-1Cr-0.7Mn. This variation in value of coefficient of expansion could be one of the reason for the under prediction of deflection value in numerical investigation from the experimental result as the value of class 40 has been used for predicting the deflection of the plate.

Table 4.2: Value of coefficient of thermal expansion as a function of temperature for Gray Cast Iron, class 40 and for 3C-2Si-1Cr-0.7Mn.

Temperature (°C)	Coefficient of thermal expansion for class 40 [22] (1/K)	Coefficient of thermal Expansion (3C-2Si-1Cr-0.7Mn) [23] (1/K)
21	.11010E-4	.10000E-4
149	.11602E-4	.12100E-4
260	.12124E-4	.14000E-4
427	.12908E-4	.16200E-4

4.6.2 Young's Modulus

The value of the Young's modulus has been shown in the Table 4.1. To check the effect of Young's modulus on the plate deflection, its value has been increased by 50% from the original value. After increasing the value of coefficient of expansion by 50%, effective deflection increases to 0.011080 mm from 0.011081 mm as shown in Table 4.2, which is only 0.009024 % more from the old value of the plate.

4.6.3 Heat capacity

The value of the heat capacity has been taken as 450.00 (J/ (Kg-K)). This value has been increased by 50% to check its effect on the deflection of the plate. After increasing the value of heat capacity, effective deflection increases to 0.011088 mm. This increase in heat capacity increases the value of the plate deflection by 0.063170 % from the old value.

4.6.4 Thermal conductivity

The value of the thermal conductivity has been taken as 450.00 (J/ (Kg-K)) from the EDU Pack Software [22]. This value has been increased by 100% to check its effect on the deflection of the plate. After increasing the value of thermal conductivity, effective deflection increases to 0.011084 mm. This increases value of the plate deflection by 0.027070 % from the old value.

4.6.5 Yield strength

The original values of the yield strength has been shown in Table 4.1. Assumed values for yield strength are obtained by increasing the original value by 50 % from the tensile test experiments. After increasing the value of yield strength by 50%, effective deflection remains same as old value, having no effect on the effective deflection of the plate.

Table 4.2 shows the effect of various material properties on the predicted effective deflection of the Safe-T Element plate. The only property that has a significant effect on the plate deflection is the coefficient of thermal expansion which increases the deflection by about 120% for doubling the value of the coefficient of expansion. The effect of all other properties is negligible.

It has also been observed that the change in the magnitude of the various material properties did not affect the location for the maximum and the minimum deflections. The

maximum and minimum deflections have always been observed at nodes 569 and 245, respectively, at a distance of 52.94 mm from the centre of plate.

Table 4.3: Effect of material properties on the predicted deflection

Property changed	% difference in material property	effective deflection with new value [mm]	effective deflection with old value [mm]	percentage difference in deflection
Co-efficient Of expansion	100	0.024414	0.011081	120.32
Young's Modulus	50	0.011080	0.011081	0.009024
Heat Capacity	50	0.011088	0.011081	0.063170
Thermal Conductivity	100	0.011084	0.011081	0.027070
Yield's strength	50	0.011081	0.011081	0

4.7 Improvement of the design of the Safe-T Element plate

In order to reduce the deflection of the Safe-T Element plate, different modifications of the current design have been proposed and simulated with the main objective of minimizing the deflection and brining its value to less than 0.1 mm as requested by Pioneering Technology Inc. It was believed that increasing the plate thickness might help in reducing the maximum deflection. However, the thickness of the plate can only be increased uniformly along the radius between the rings because any other way will make fixing of the heating element on the Safe-T Element plate more difficult

The following four suggested modifications have been considered to reduce the plate maximum deflection:-

- Increasing the thickness uniformly along the radius of the Plate.
- Increasing the thickness of the centre section (the distance from the centre to the inner ring of plate) and the thickness of rest of the plate by different ratios.
- Keeping the centre section the same and changing the thickness of the rest of the plate
- Decreasing the thickness of the centre section and increasing the thickness of rest of the plate.

Table 4.3 shows the results of the numerical simulations of the fourteen different cases considered to improve geometry for the Safe-T Element plate. Results indicate reduction in the deflection ranging from 7.48% by uniformly increasing the thickness of plate by 10% to 81.42% reduction in the value of the deflection by removing the outer ring from the current design of the Plate. Figure 4.8 shows the current design of Safe-T Element plate.

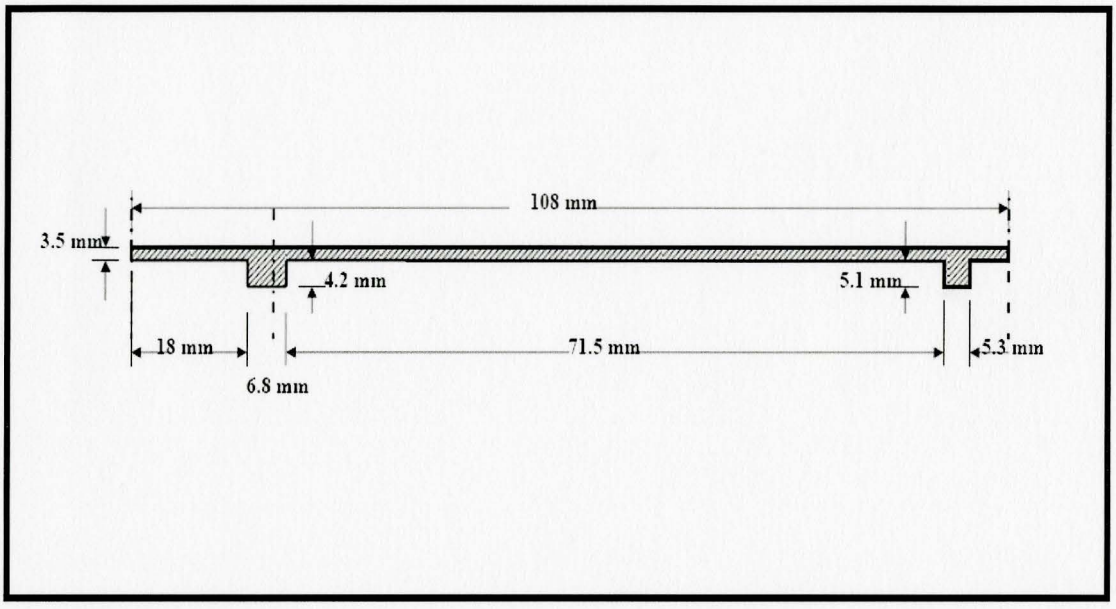

Figure 4.8: Half section of current design of Safe-T Element, showing inner and outer ring.

The results of these proposed modifications are shown in Figures 4.9 to 4.22. Figure 4.22 shows that by just removing the outer ring of the plate and keeping all other dimensions as in original design, the value of the deflection decreased to 0.0213585 mm, which is 81.4% less than the current design. This means that the measured deflection of 0.35 mm in the experiments with this modification can be reduced to 0.0686 mm, which is lower than the maximum deflection (0.1 mm) recommended by PTI. Figure 4.23 shows the value of deformation along the radius of the plate for current design, 10 and 20% uniform increase in the thickness of the plate.

Table 4.4: Result of the simulation by changing the geometry of the plate from the current design.

Case No.	Proposed Modification	Maximum Deflection [mm] with current design	Maximum Deflection [mm] modified geometry	% Decrease in deflection
1	Thickness increased uniformly by 10 %	0.114985	0.106373 7	7.48
2	Thickness increased uniformly by 20 %	0.114985	0.0994787	15.58
3	Center section thickness increased by 60 % and the rest by 30%	0.114985	0.0948648	17.49
4	Thickness increased uniformly by 50 %	0.114985	0.0832386	27.6
5	Centre section thickness is at its original and the rest increased by 30%	0.114985	0.0701056	39.03
6	Centre section thickness decreased by 30% and the rest increased by 30%	0.114985	0.0678940	40.95
7	Centre section thickness decreased by 13% and the rest increased by 53 %	0.114985	0.0561552	51.16
8	Centre section thickness decreased by 4% and the rest increased by 63 %	0.114985	0.0525665	54.28
9	Centre section thickness increased by 5%and the rest increased by 73 %	0.114985	0.0502577	56.29
10	In the Centre section thickness increased by 18%and the rest increased by 83 %	0.114985	0.0476427	58.56
11	Centre section thickness original and the rest increased by 83%	0.114985	0.0473728	58.80
12	Centre section thickness increased by 26%and the rest increased by 93 %	0.114985	0.0464792	60
13	Centre section thickness increased by 57%and the rest increased by 123 %	0.114985	0.0444345	61.35
14	No outer ring, keeping original dimension	0.114985	0.0213585	81.42

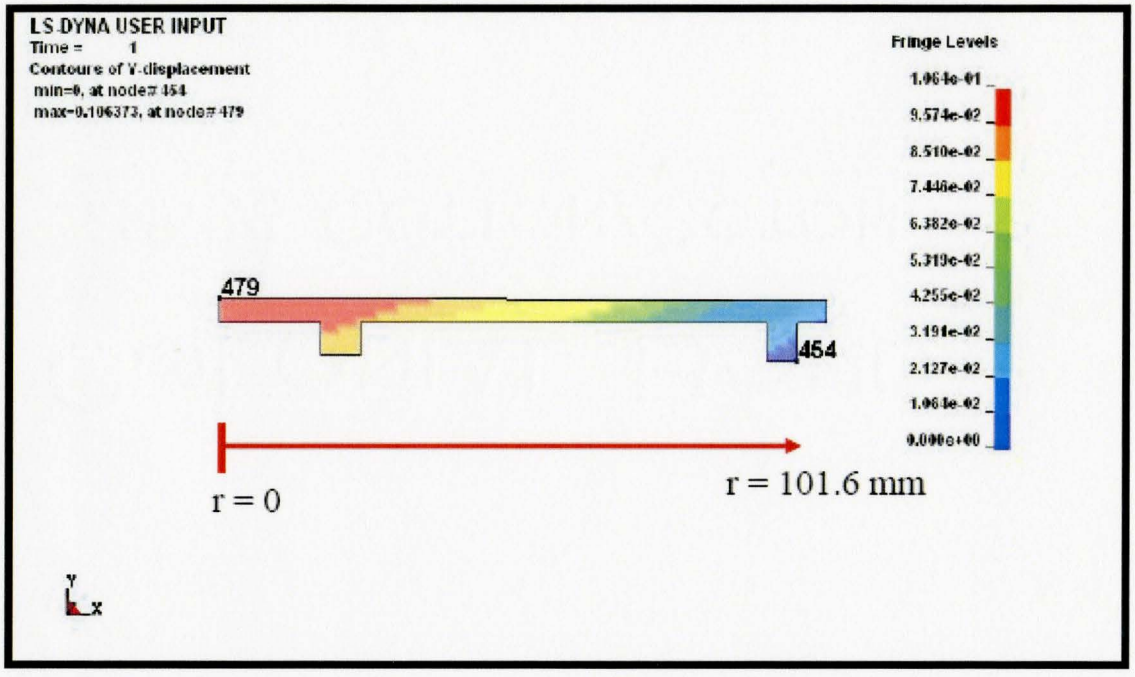

Figure 4.9· Deflection profile for case 1 of Table 4.3

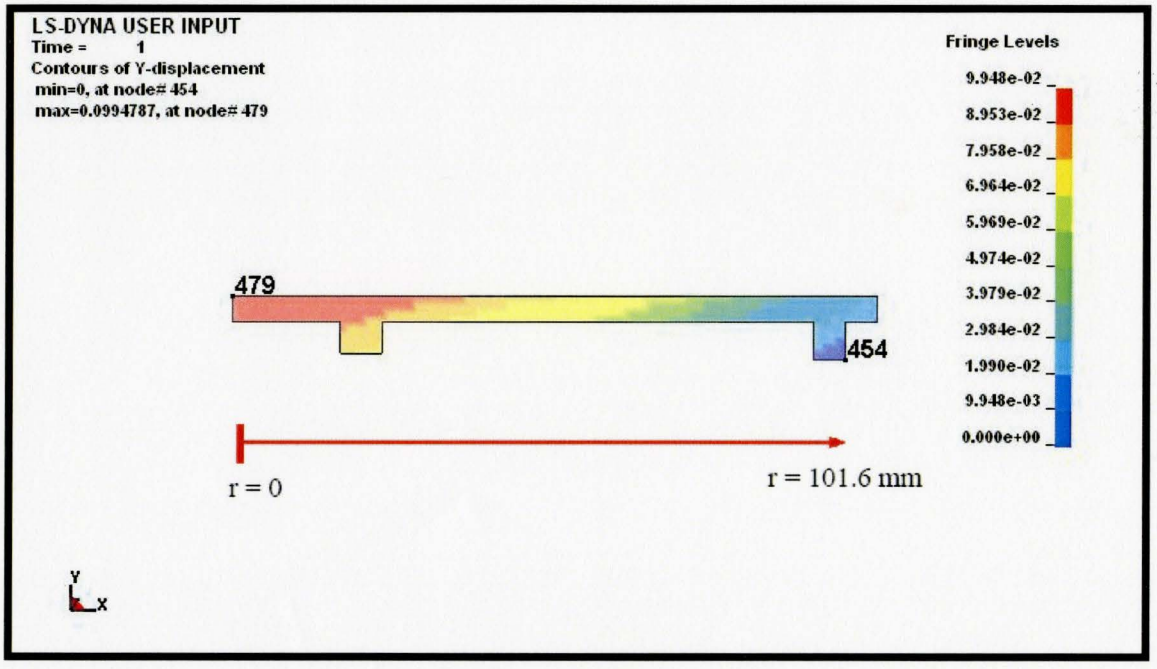

Figure 4.10· Deflection profile for case 2 of Table 4.3

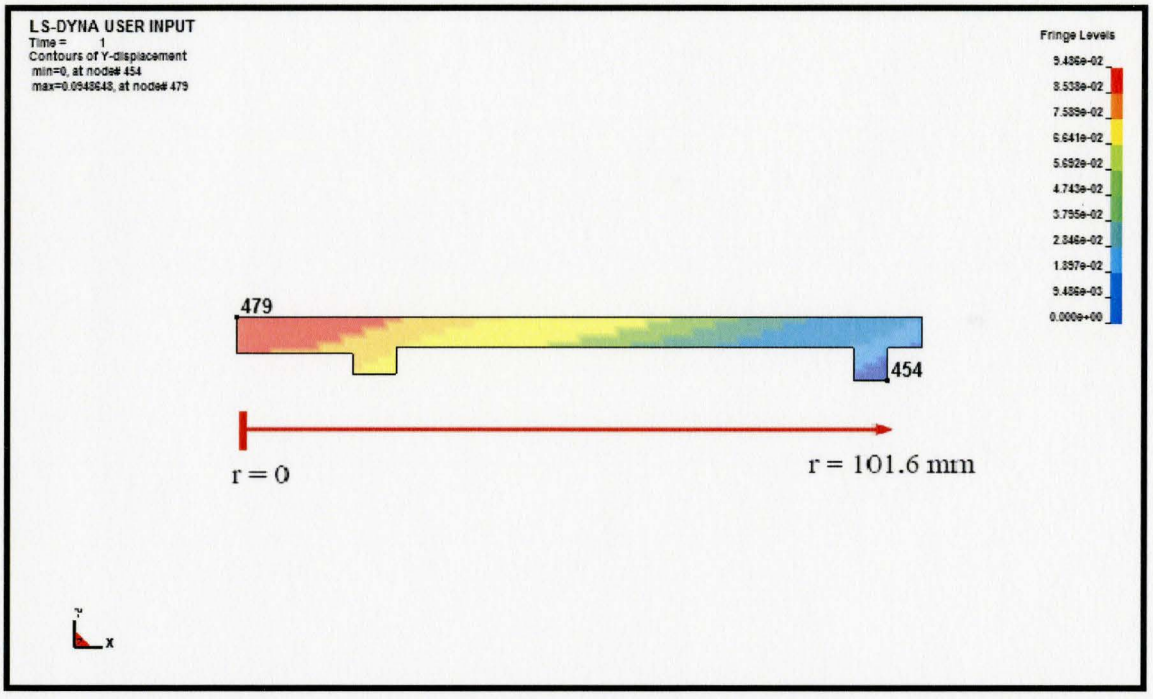

Figure 4.11 Deflection profile for case 3 of Table 4.3

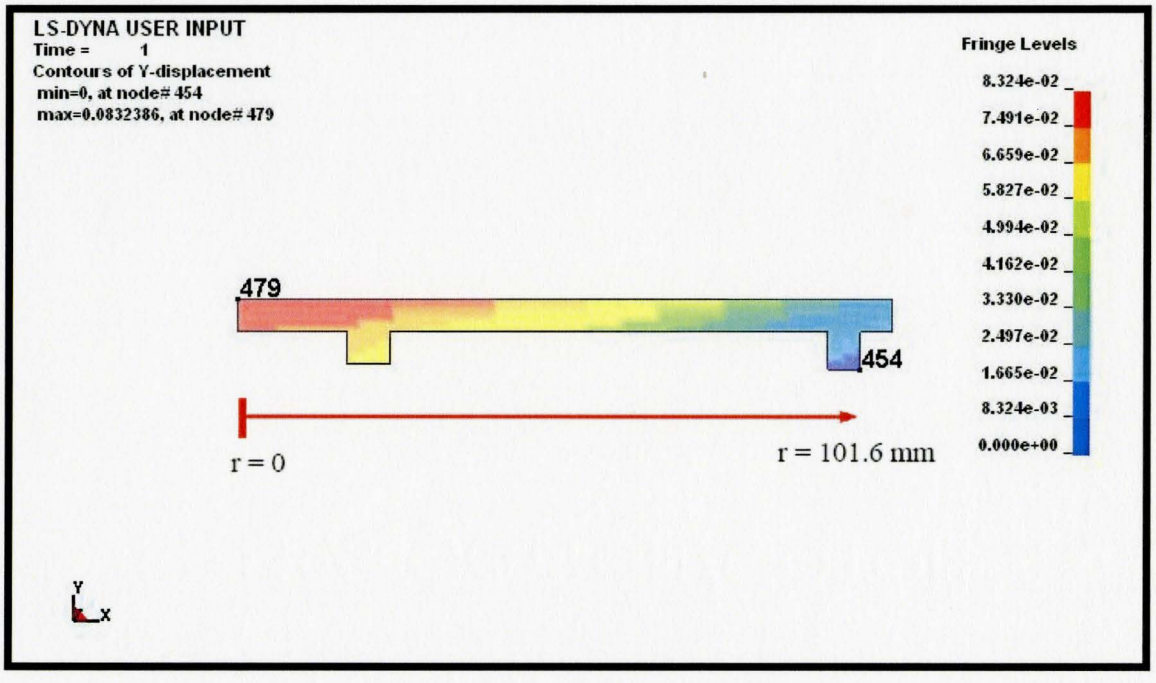

Figure 4.12. Deflection profile for case 4 of Table 4.3

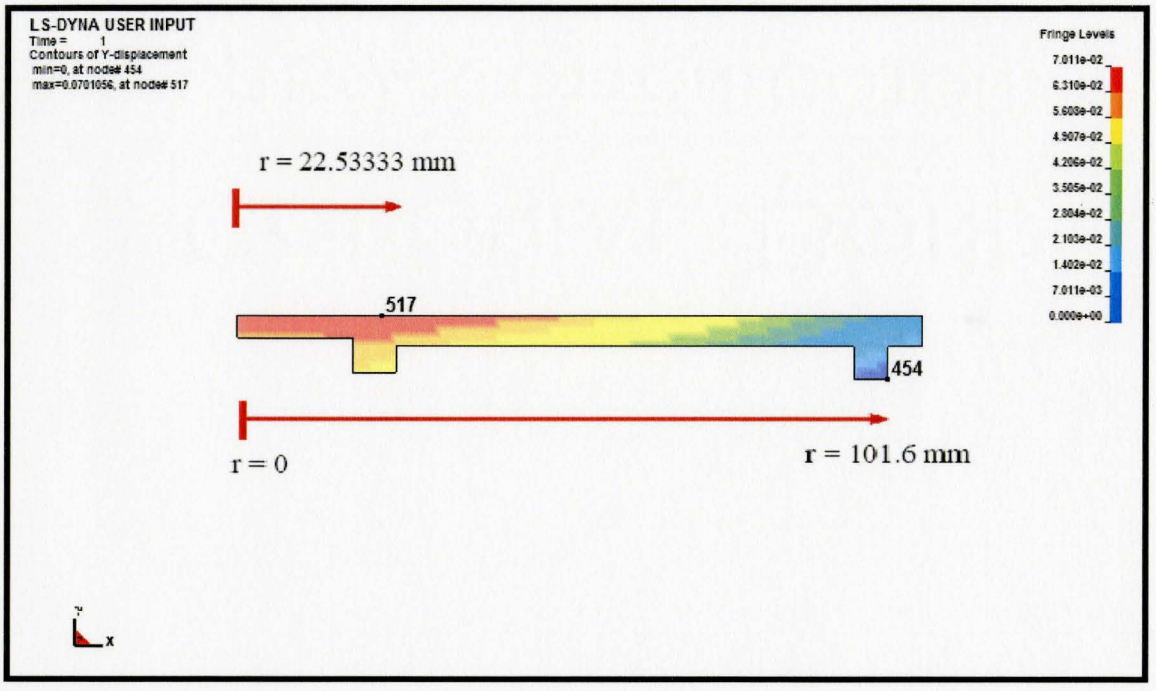

Figure 4.13 Deflection profile for case 5 of Table 4.3

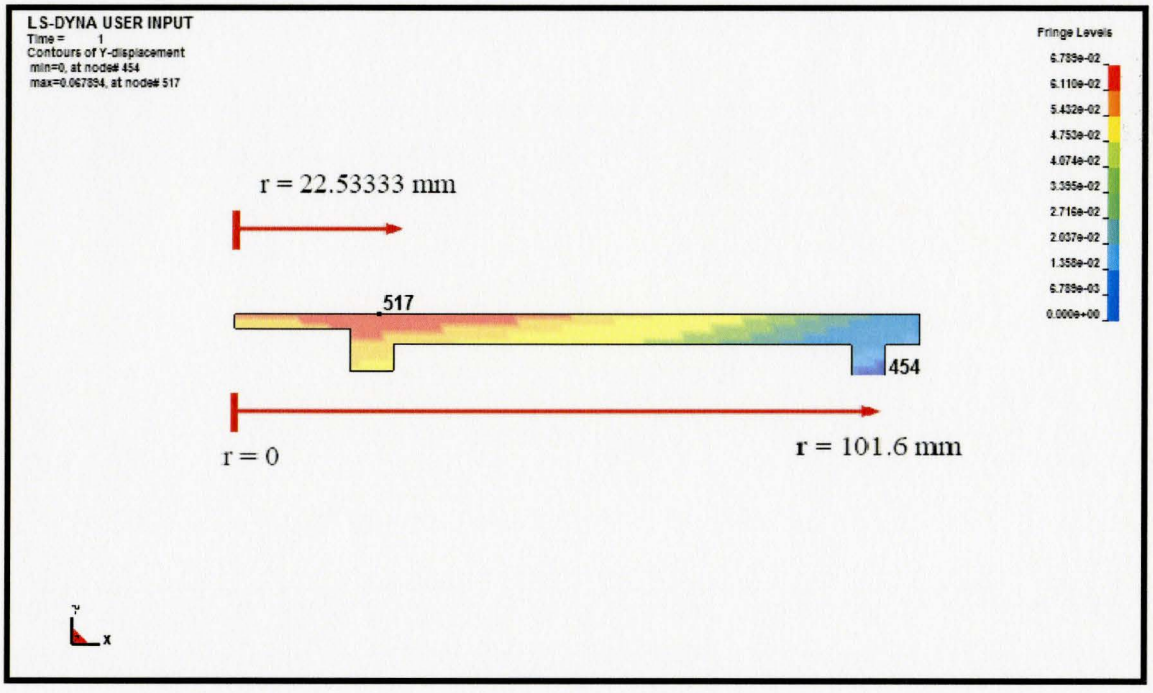

Figure 4.14: Deflection profile for case 6 of Table 4.3

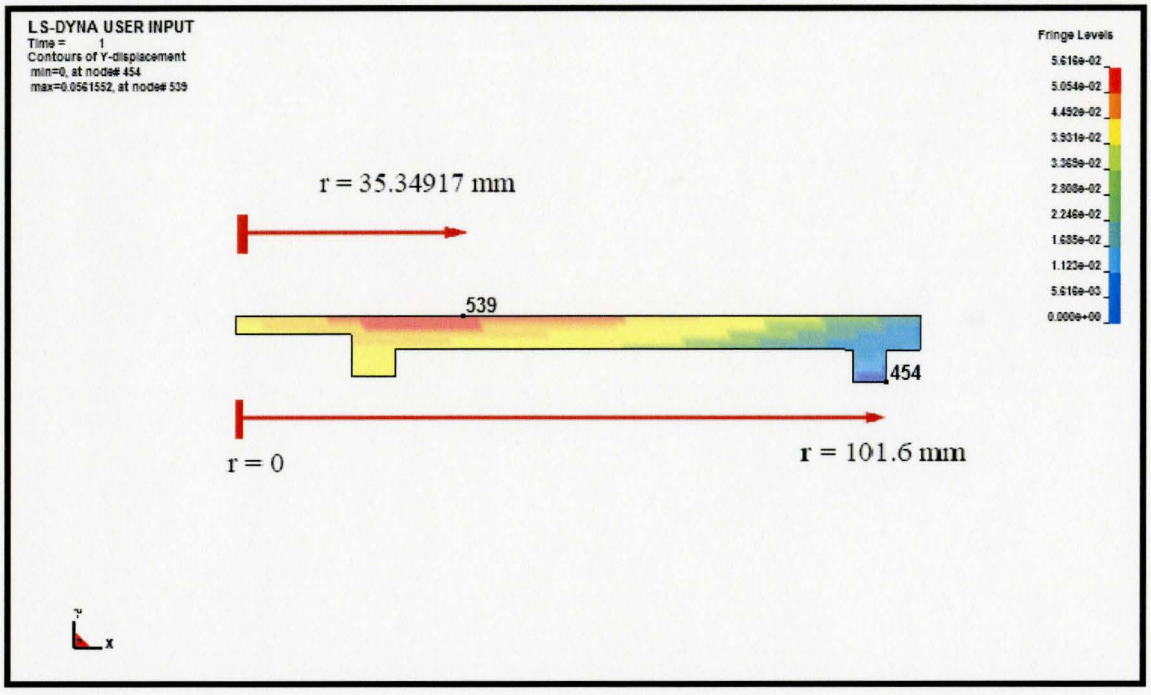

Figure 4.15 Deflection profile for case 7 of Table 4.3

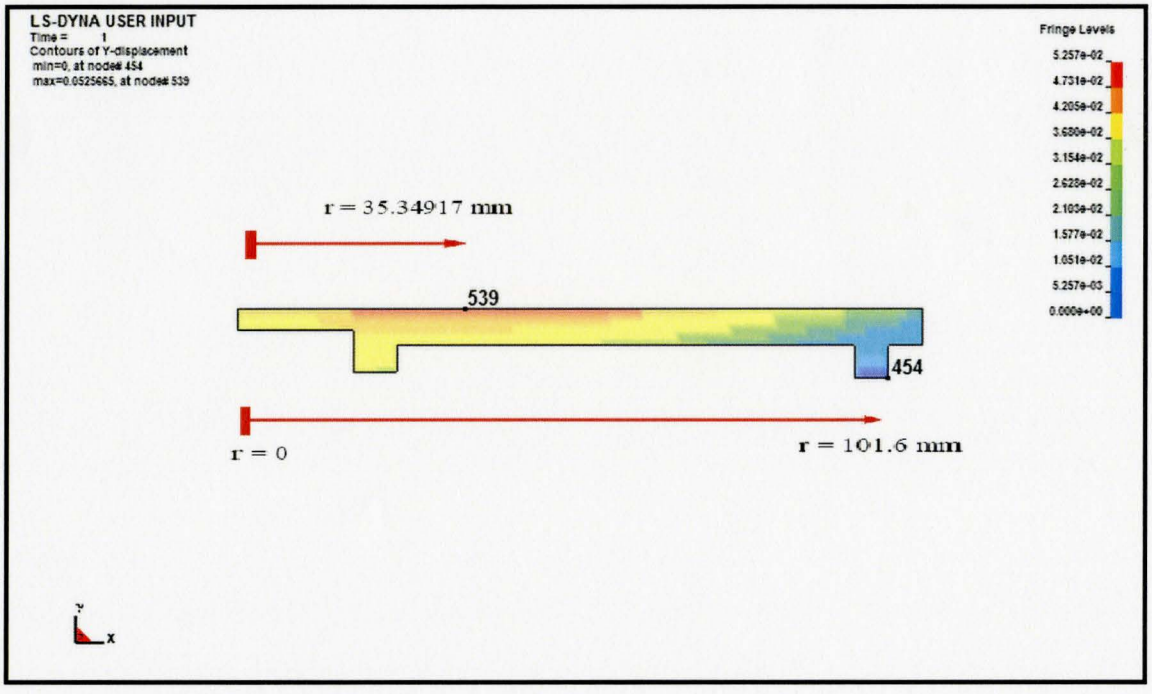

Figure 4.16: Deflection profile for case 8 of Table 4.3

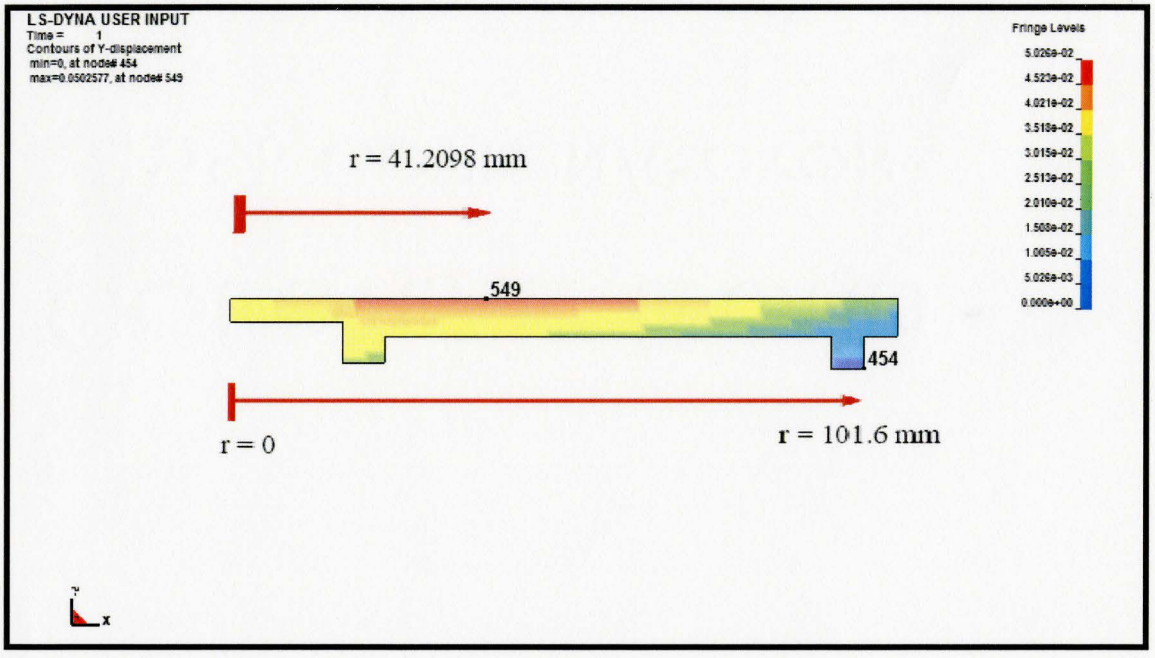

Figure 4.17 Deflection profile for case 9 of Table 4.3

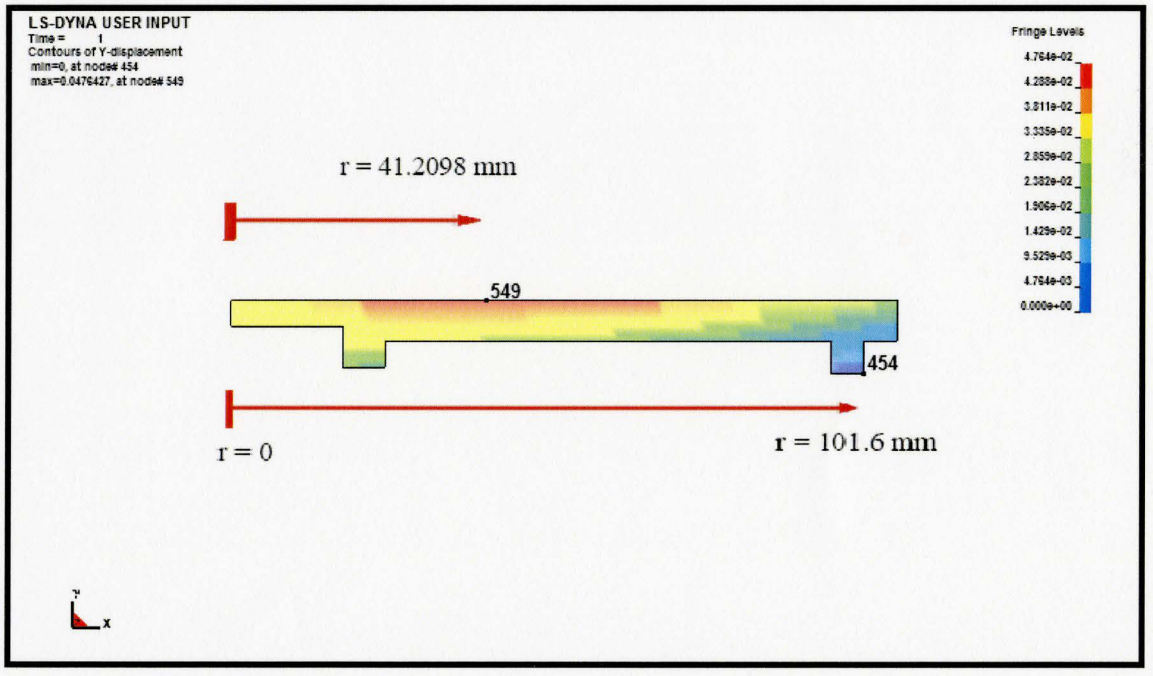

Figure 4.18 Deflection profile for case 10 of Table 4.3

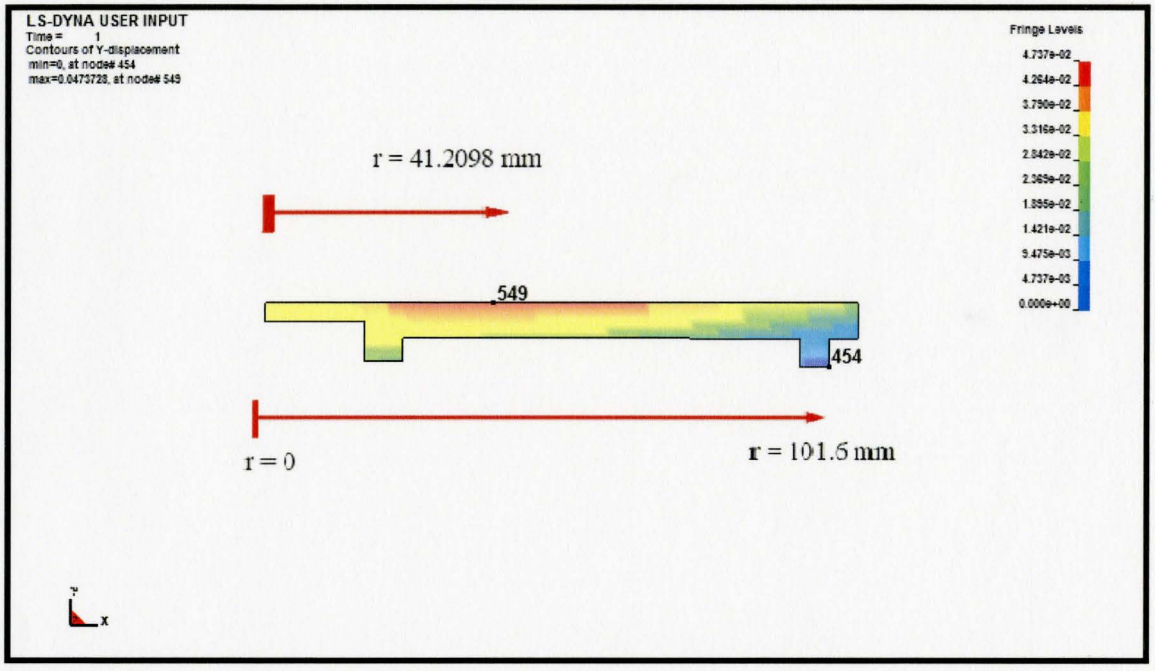

Figure 4.19· Deflection profile for case 11 of Table 4.3

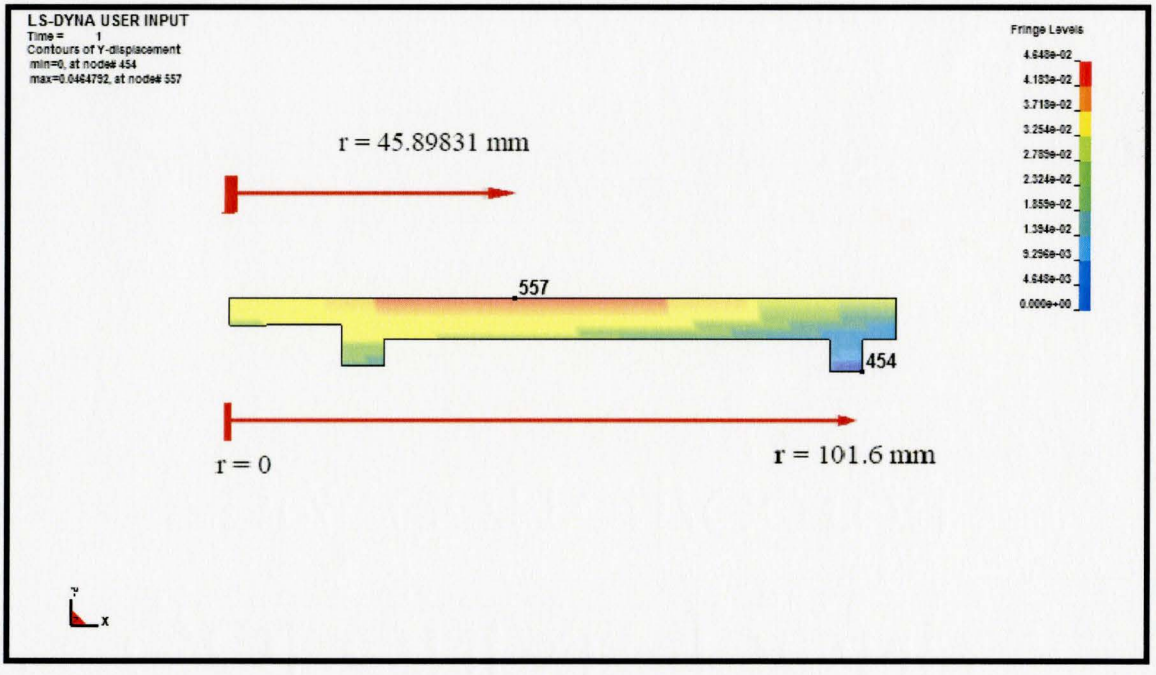

Figure 4.20: Deflection profile for case 12 of Table 4.3

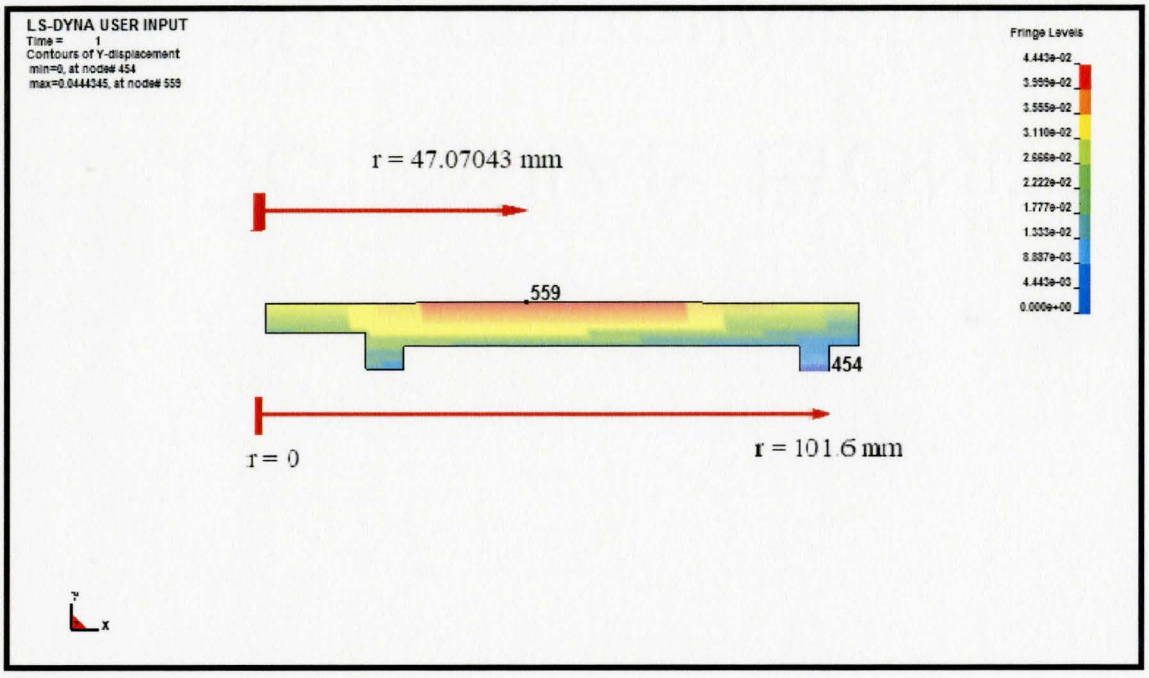

Figure 4.21 Deflection profile for case 13 of Table 4.3

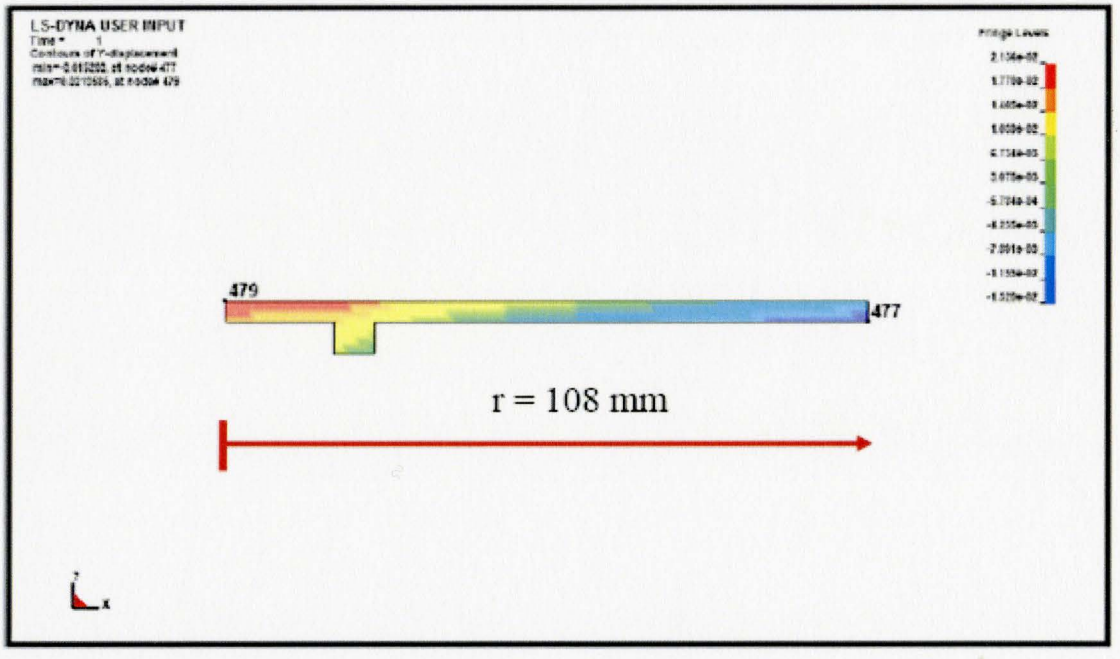

Figure 4.22. Deflection profile for case 14 of Table 4.3

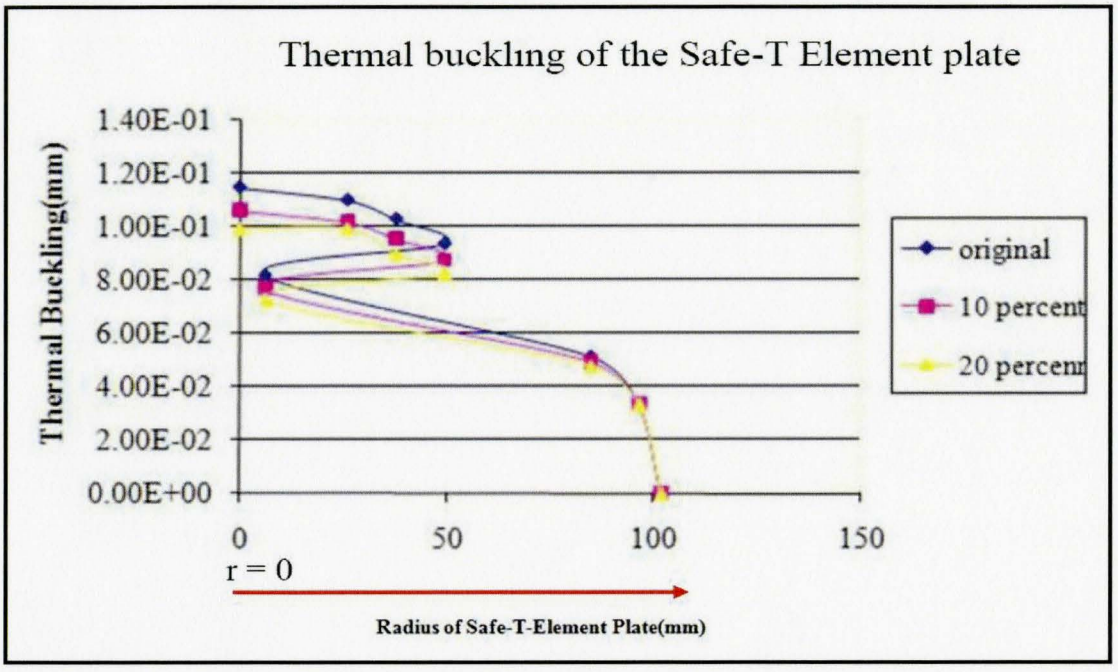

Figure 4.23 Graph showing value of deformation along the radius of the Safe-T Element plate for original geometry, 10 and 20% uniform increase in the thickness along the radius.

4.8 Proposed Design for the Safe-T Element plate for minimum deflection

Proposed design for the Safe-T Element plate is shown in Figures 4.24 and 4.25 This design has been proposed by removing outer ring from the current design of the Safe-T Element plate based on the simulation results of the previous section in the Table 4.3

Three brackets on the bottom of the Plate have been added to support clips for mounting the Radiant heating element.

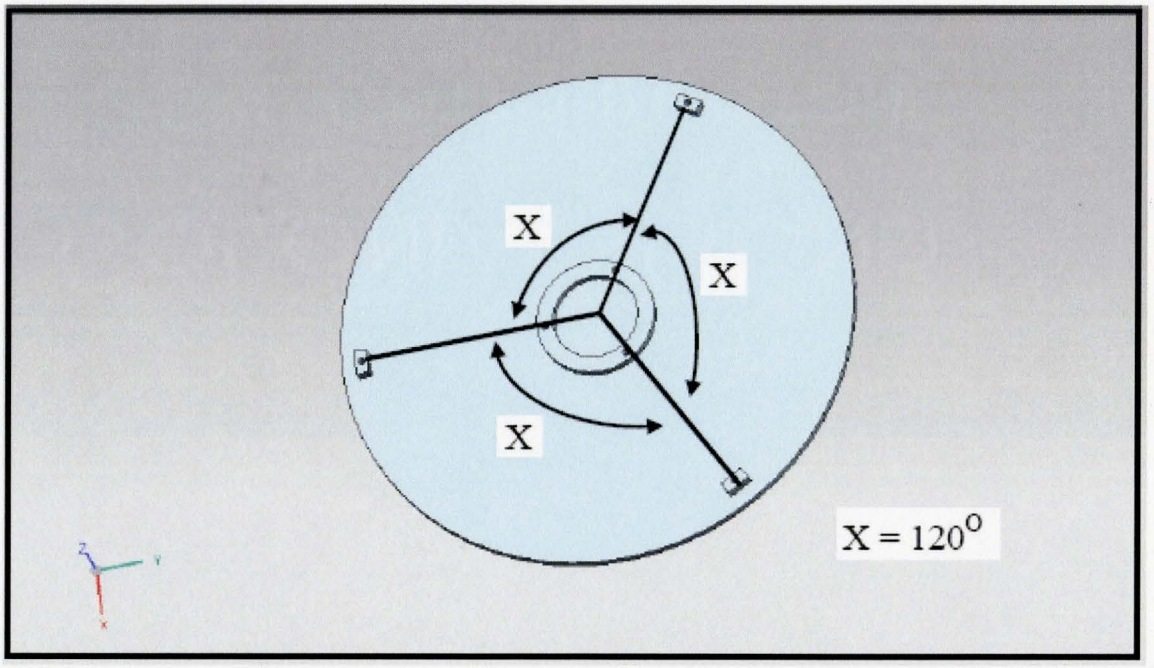

Figure 4.24: The proposed design for the Safe-T-Element Plate, case14 in Table 4.3

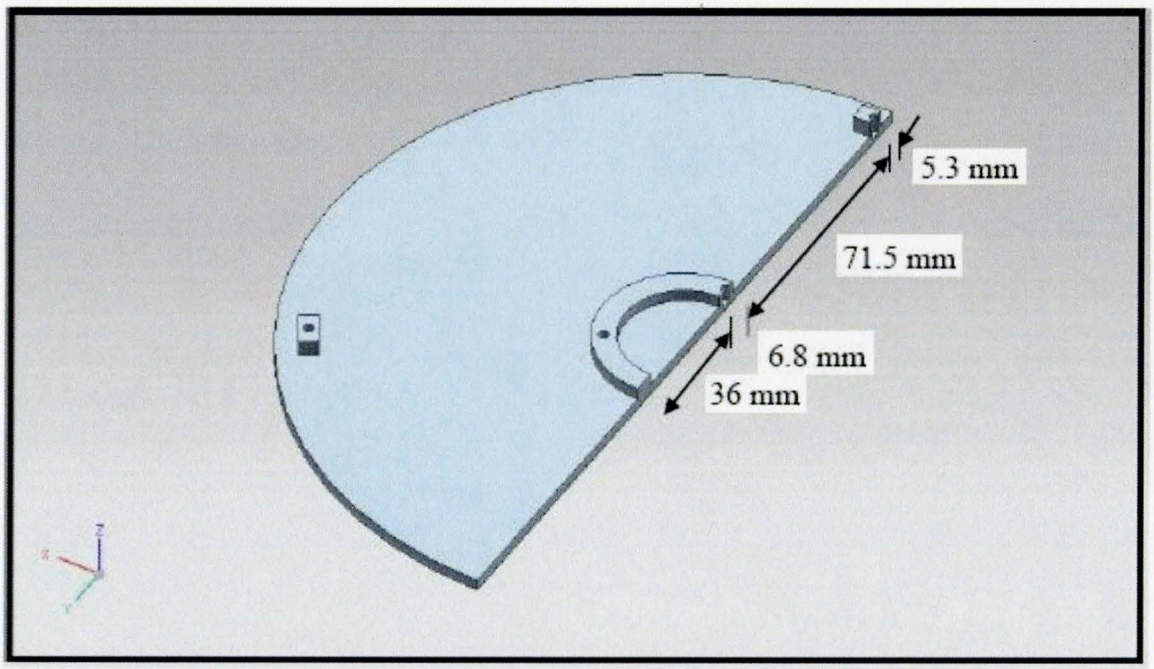

Figure 4.25 Section view of the proposed design.

Chapter 5

5 Summary, Conclusions and Future Work

5.1 Summary

The problem of thermal buckling (deflection) of the Safe-T Element plate due to non uniform temperature profile generated by the heating element of a conventional stove has been investigated experimentally and numerically.

The present study has been started with little information about the type of Safe-T Element plate. Chemical analysis has been first performed to obtain the chemical composition of the material. The chemical analysis alone is not enough to provide sufficient information about the type of cast iron used as there are four main types of cast iron available, so microstructure and tensile testing have been performed to determine the type and grade of the cast iron used.

Differential Scanning Caleromitry testing has been performed to examine thermal stability of the material. Tests have been also performed to check whether the internal stresses are the cause of the distortion of the plate.

Transient temperature distribution of the Safe-T Element plate in both the radial and the circumferential directions as well as the deflection have been measured. Result indicated that the deflection problem of the Safe-T Element plate is due to thermal buckling.

Two dimensional numerical investigations have been performed to first study the effect of material properties on the thermal buckling of the Safe-T- element plate and to examine some proposed geometry design that would reduce the deflection to its maximum allowable limit.

5.2 Conclusions

1. The material of the Safe-T Element plate is a homogenous and thermally stable Gray Cast Iron
2. Based on present tensile test results and information found in the literature, the grade of gray cast iron used for the Safe-T Element can be assumed as class 40.
3. Residual stresses are not the cause of the distortion problem of the Safe-T Element plate. The problem is due to elastic thermal buckling.
4. The maximum deflection from both the experiments and the numerical simulations occurred at the centre of the plate.
5. The coefficient of thermal expansion was found to have the most significant effect on the plate deflection, while the effect of other properties is negligible. This indicated that the problem is mainly due to thermal elastic deformation.

6. Changing the values of various material properties did not affect the location of the maximum and minimum deflection on the plate
7 The deflection of the plate was reduced by increasing the thickness. The location of the maximum deflection also changed with the increase in the thickness of the plate. The measured maximum deflection was 0.35 mm compared with 0.12 mm from the simulations. This difference can be attributed to the following reasons.
    - The material is not exactly grade 40 of Gray Cast Iron.
    - The plate temperature varies in both the circumferential and the radial directions, so averaging the temperature in one direction is an approximation.
    - The uncertainty in measuring the temperature and deflection of the plate could be possible reasons for the difference between the experimental and numerical values.
8. Though deflection can be reduced by increasing the thickness of the plate, but it will increase the cooking time with same heat inflow from the heating coil.
9 Deflection can be minimized by removing the outer ring from the present design

5.3 Future Work

Three-dimensional simulations should be carried out in order to account for temperature variation in the radial and circumferential directions.

Bibliography

[1] http://www.pioneeringtech.com/

[2] Walton and Charles F.,"The Gray Iron Casting Handbook: Including Data on Gray, Ductile, White and High Alloy Irons, Gray Iron founder's society", Cleveland 1958.

[3] Haenny L. and Zambelli.G., "The Stiffness and Modulus of Elasticity of Grey Cast Iron", Journal of Material Science Letters V2, pp.239-242, 1983

[4] Callister, "Fundamentals of Materials Science and Engineering-An Interactive Text," John Wiley & Sons, New York 2001

[5] Rourke O R., "Cast Iron. The Engineering Metal", Advanced Material and Process, January pp.65-69, 2001

[6] Bazdar M., Abbasi H.R., Yaghtin A. H. and Rassizadehghani J., "Effect of Sulpur on Graphite Aspect Ratio and Tensile Properties in Compacted Graphite Irons", Journal of Material Processing Technology, 209, pp.1701-1705, 2009

[7] Helsing J and Grimvall G., "Thermal Conductivity of Cast Iron. Models and Analysis of Experiments", Journal of Applied Physics, 70(3), pp. 1198-1206, 1991

[8] Abbasi. H. R, Bazdar M and Halvaee. A., "Effect of Phosphorous as an Alloying Element on Microstructure and Mechanical Properties of Pearlitic Gray Cast Iron", Material science and engineering A 444, 314-317, 2007

[9] De Garmo, Ernest P., "Material and Process in Manufacturing",. John Wiley & Sons, New York, 1999

[10] Pollack, Iron Carbon Phase Diagram, Fe-Fe3C Phase Diagram, Materials Science and Metallurgy, 4th ed., Prentice-Hall, 1988.

[11] Willidal. T, Bauer W and Schumacher P, "Stress/Strain Behaviour and Fatigue Limit of Grey Cast Iron", Material Science And Engineering A 413-414, 578-582, 2005

[12] Geier G. F, Bauer W, Mckay B. J and Schmacher P., "Microstructure Transition from Lamellar to Compacted Graphite using Different Modification Agents", Material Science And Engineering A, 413-414,pp. 339-345, 2005

[13] Alvarez L, Luis C., J and Puertas I., "Analysis of The Influence of Chemical Composition on the Mechanical and Metallurgical Properties of Engine Cylinder Bocks in Grey Cast Iron", Journal of Material Processing Technology 153-154, pp 1039-1044, 2004.

[14] Anon, "Mechanical Properties of Gray Iron", Engineered casting solutions, 6(3) 30-32, 2004

[15] Wei W, Tianfu J, Yuwei G , Guiying Q and Xin Z, "Properties of a Gray Cast Iron with Oriented Graphite Flakes", Journal of Material Processing Technology 182 593-597, 2007

[16] Bertodo R., "Grey Cast Irons for Thermal-Stress Applications", Journal of Strain Analysis V5 no 2,pp 98-108, 1970.

[17] Masatoshi T., "Characteristic of Thermal Expansion and Oxidation at high Temperature of Cast Iron with Different Graphite Shapes", Technology reports of kansi university V 25, 111-124, 1984.

[18] Hecht R. L., Dinwiddie R. B and Wang H, "The Effect of Graphite Flake Morphology on the Thermal Diffusivity of Gray Cast Irons Used for Automotive Brake Discs", Journal of Material Science 34., pp. 4775-4781, 1999

[19] Kohout J., "A Simple Relation For Deviation of Grey and Nodular Cast Irons from Hooke's Law", Material Science and Engineering, A 313., 16-23, 2001

[20] Graciela B. and Juan E., "Geometrical Effect on Lamellar Grey Cast Iron Fracture Toughness", journal of material processing technology 179, 202-206, 2006.

[21] Kalkani. A, Uysal. I and Guldur H, "The Analysis of Cooling Curves for Grey Cast Iron and its Mechanical Properties, Canadian Metallurgical quarterly", 42, 343-348, 2003

[22] EduPack Software, GRANTA Design Limited, U K.

[23] MPDB Software, Version 6.51, JAHM Software Inc. U.S.A.

[24] Gray and Ductile Iron Casting Handbook, The Gray and Ductile Iron Founder's Society Inc., R. R. Donnelley & Sons Company, Cleveland, 1971